Journal Pre-proof

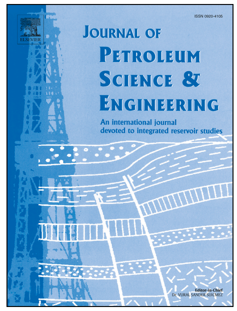

The identification of normal to underpressured formations in the Southeastern Sichuan basin

Melckzedeck Michael Mgimba, Shu Jiang, Grant Charles Mwakipunda

PII: S0920-4105(22)00937-8

DOI: https://doi.org/10.1016/j.petrol.2022.111085

Reference: PETROL 111085

To appear in: *Journal of Petroleum Science and Engineering*

Received Date: 23 November 2021

Revised Date: 9 September 2022

Accepted Date: 24 September 2022

Please cite this article as: Mgimba, M.M., Jiang, S., Mwakipunda, G.C., The identification of normal to underpressured formations in the Southeastern Sichuan basin, *Journal of Petroleum Science and Engineering* (2022), doi: https://doi.org/10.1016/j.petrol.2022.111085.

Melckzedeck Michael Mgimba

Methodology, software, analysis, writing the original manuscript, writing the second draft (revised)

Shu Jiang

Conceptualization, validation, editing the manuscript (original and revised) and supervision

Grant Charles Mwakipunda

Validation and editing the manuscript

The Identification of Normal to Underpressured Formations in the Southeastern Sichuan Basin

Melckzedeck Michael Mgimba[1,2], Shu Jiang[1*], Grant Charles Mwakipunda[1]

1. **Key Laboratory of Tectonics and Petroleum Resources of Ministry of Education, China University of Geosciences, Wuhan, 430074, China**
2. **Mbeya University of Science and Technology (MUST), P.O Box 131, Mbeya, Tanzania**

*** Corresponding author: Key Laboratory of Tectonics and Petroleum Resources of Ministry of Education, China University of Geosciences, Wuhan, 430074, China**

E-mail address: jiangsu@cug.edu.cn (S. Jiang)

Abstract

The Sichuan Basin contains many overpressured formations with pore pressure coefficients as high as 2.3. However, in a Nanye 1 well found in the Southeastern (SE) Sichuan Basin, low-pore pressure coefficients as low as 0.9 have been recorded at a depth between 1544.3 and 1903.6 m, indicating the presence of underpressured formations. But the knowledge of normal and underpressured formations is not well studied in the SE Sichuan Basin. In this work, the normal to underpressured formations in the SE Sichuan Basin are identified, and their origins are discussed.

We integrated the pore pressure measurement and estimation, pore pressure coefficient and pore pressure depth plot to identify the normal to underpressured formations. We also integrated basin modelling along with the faults system to determine the origins of underpressured formations. As a result, the Upper Permian Longtan and Middle Permian Maokou Formations (1906.5-2782.9 m depth) in the Nanchuan area, were identified as normal-to-underpressured gas deposits. Also, the study identified the Lower Silurian Longmaxi and Upper Ordovician Wufeng Formations (2072-2160 m depth) in the Pengshui area, SE of the Chongqing region as normal pressured gas formations. The study discovered a decrease in temperature, rock porosity rebound and gas migration out of the formations through faults as the reasons for underpressured formations in this area. The tectonic uplift and erosion resulted in a decrease in temperature and rebound of the rock porosity, which contributed to total pore pressure drop up to 46.62 MPa. The tight overlying seal rocks and underlying rocks helped to sustain the low pore pressures in these formations.

1. Introduction

The increase in gas and oil demand and depletion of the matured gas and oil fields attract petroleum experts to put their eyes on the underpressured reservoirs (Dasgupta and Mukherjee, 2020). The underpressured reservoirs have formation pore pressures less than the hydrostatic pressure. Whereas the higher-pore pressure formations are called overpressured formations, and normal pressured formations have formation pore pressures equal to hydrostatic pressure. According to Duan and Wu (2020), the number of underpressured oil and gas fields in the world is large. By 1995 it was approximated that 11.7% of the 160 worldwide oil and gas fields were underpressured and about 15.7% of the 210 worldwide gas fields were underpressured gas fields. Currently, there are many known underpressured reservoirs in the world, e.g., Palaeozoic gas reservoirs in Alberta Basin, Canada, the Palaeozoic gas reservoirs in Denver Basin, USA, and the Mesozoic gas reservoirs in Ordos Basin, China, which have pore pressure coefficients ranging from 0.7 to 0.9 (Wang et al., 2021). The presence of underpressure in the formation influences hydrocarbon generation, migration and accumulation (Hunt, 1990). Therefore, identifying the location and origins of underpressured formations is very significant in the exploitation of gas or oil reservoirs.

Many studies have been done to analyse the origins of underpressured formations through geological analysis, geophysical analysis and numerical simulation. Erosional unloading, rock dilatancy and temperature decrease are termed as the origins of underpressure in the formations (Andreotti and Pouliquen, 2013; Barker, 1972; Bradley, 1975; Dickey and Cox, 1977; Duan and Wu, 2020; Hao et al., 2011; Nedderman, 2005; Neuzil and Pollock, 1983). But also, the migration of gases out of a formation through faults can reduce the formation volume and then causes underpressure in the formation (Law and Dicknson, 1985; Liu and Xie, 2002). Groundwater movement and the effect of osmosis are other origins of underpressure in the formations (Nelson, 2012; Serebryakov et al., 2002; Sorenson, 2005). The analysis of these factors shows that different underpressured formations have different origins.

The Sichuan Basin has a great potential for natural gas, which is approximated to be 626 trillion cubic feet (Tcf) of technically recoverable shale gas resources (Jiang et al., 2016). Although China has great potential for natural gas, they are the larger importer of gas (Lin and Wang, 2012; Wang et al., 2020). According to CHINA DATA, in 2021 natural gas imports in China increased by 20%. This indicates that the demand for natural gas in China is huge and there is a necessity to exploit both overpressured, normal pressured and underpressured hydrocarbon formations. The basin has several discovered gas fields, which are dominated by overpressured formations having pore pressure coefficients up to 2.3 (Hong et al., 2018; Lei et al., 2019; Li et al., 2016; Liu et al., 2016; Liu et al., 2016; Wang and Zhu, 2020; Xie et al., 2009; Yang et al., 2003; Yang et al., 2016; Zeng, 2010). However, some wells, including the Nanye 1 and Pengye 1 wells in the SE Sichuan Basin, have a complex pore pressure distribution. The pore pressure coefficients in the Nanye 1 well at 1544.3-4410.7 m depth range from 0.9 to 1.45 and in the Pengye 1 well at 2072-2160 m depth is 1.06. These coefficients indicate the presence of normal and underpressured formations in this area. So far, no research has been done on the (i) identification of normal and underpressured gas formations, and (ii) the origins of underpressured formations in the SE Sichuan Basin.

Although the underpressured formations are few in Sichuan Basin, the targeted gas formations are rich in organic matter. When both underpressured, normal pressured and overpressured formations in Sichuan Basin are produced, they will be able to produce about 60% of China's natural gas imports (Wang, 2020; Zhao et al., 2021). This work aims to bridge the mentioned gap in research by identifying normal and underpressured formations and studying the origins of underpressured formations.

We integrated the pore pressure measurement and estimation, pore pressure coefficient evaluation and pore pressure depth plot techniques to identify the normal to underpressured formations. Also, we applied basin modelling, faults system knowledge and mathematical models to determine the origins of underpressured formations. The identification of normal and underpressured formations and their origins will be useful to production engineers in extracting natural gas. Engineers can use this knowledge in designing the natural gas production system, including planning compressors' capacity or diameter of production pipes. Also, the study will help engineers design the methods of boosting formations' pore pressure, such as water flooding.

2. Geological setting

This study was conducted in the Chongqing region (Nanchuan area and SE of Chongqing region)-east of the Sichuan Basin (Fig. 1) and has an area of approximately 1.98×10^4 km^2. The SE of the Chongqing area consists of two parts, Eastern Sichuan ejective fold belts and the Western Hubei-Eastern Chongqing trough fold belts (Jing et al., 2016). Sichuan Basin is located in the Southwest of China. The basin is part of the Yangtze Platform, which is located in the northwestern. It is a huge, intracratonic basin sitting on the stable south China Block. The Sichuan Basin has a large area of approximately $23 \times 10^4 km^2$. The basin was formed in the late Proterozoic and extends to the present (Korsch et al., 1991; Liu et al., 2017). In the middle of the basin, the basement contains intermediate basite magmatic rocks that have experienced strong metamorphism (Zhili, 1998). The Sichuan Basin is surrounded by mountains on both sides. In the north, south, west and east, the basin is surrounded by Micang and Daba, Daliang, Longmen, and Dalou mountains, respectively (Xu et al., 2018).

The stratigraphy of the Southeastern Sichuan Basin

The stratigraphy shows that the SE Sichuan Basin experienced several tectonic movements including Caledonian, Indosinian, Yanshanian and Himalayan. The region consists of several formations with successions zones of clastic rocks (shale, sandstone and mudstone) and carbonate rock (limestone) (Fig. 2). These rocks were deposited during the tectonic evolution stages. Those tectonic evolution stages include cratonic depression and a foreland basin, which occurred in the Palaeozoic and Triassic Eras, respectively (Shu-Gen et al., 2016). In the craton stage, the marine carbonate rocks were deposited. The terrestrial clastic rocks were deposited during the foreland basin stage (Yi-Feng et al., 2015). Therefore, these tectonic evolution stages caused the region to comprise interbedded formations of clastic beds and carbonate beds (Feng et al., 2003; Guo et al., 2011; Wang, 2003). In addition, the tectonic disruptions generated many faults and unconformities, which caused hydrocarbon migration and gas preservation (Shugen et al., 2012). Other thrust faults formed in the region, in the Early to Middle Jurassic, due to the squeezing of the region. The stress regime of those thrust faults turned from extrusion to extension during the Cretaceous. But due to the influence of the intrusion of the India-Australian plate onto the Eurasian plate, the stress regime changed again from extension to extrusion in the Neogene (Wo et al., 2007).

Several series of tectonic uplifts and erosions happened in this region. The first tectonic uplift and erosion happened during the Devonian and Carboniferous periods. The major erosion happened during the Permian and Early Triassic. Another tectonic uplift happened in the late Triassic and during this time the collision between the North China Plate and the South China plate happened (Qi et al., 2015; Wang et al., 2015). The tectonic uplift exposed some underlying formations on the surface, and the erosion removed the exposed surface. Hence, the tectonic uplift and erosion caused the absence of some formations in the basin (Yi-Feng et al., 2015).

The main source rocks in this region are Longmaxi, Wufeng, Longtan and Maukou as shown in Fig. 2. The Longmaxi shale was deposited in the deep-sea shelf sedimentary environments in the Early Silurian period. This happened when shale experienced deep burial in the Yanshan period. But the occurrences of tectonic uplift and erosion caused the hydrocarbons to migrate out of the formation (Hailong et al., 2012). The Wufeng shale formed in the Late Ordovician period in the foreland basins due to the foreland uplifts that occurred in the orogenic belts (Jing et al., 2016).

3. Methodology

To conduct this study, different approaches were used. In identifying the normal to underpressured formations, we used pore pressure measurement, pore pressure evaluation and pore pressure depth analysis. Whereas the basin modelling, evaluation of the effect of uplift and erosion by the mathematical model and studying the effect of faults system in the region were used in studying the origins of underpressured formations.

3.1. Pore pressure evaluation

The process of evaluating the pore pressure system in the Chongqing region was conducted by the following different approaches including direct pore pressure measurement, pore pressure coefficient evaluation and pore pressure depth relationship analysis.

3.1.1. Pore pressure measurement

The formation pore pressures were measured by using the drill stem tests (DSTs). In the DSTs, fluid flowed from the formation to the drilling pipe and then to the surface. The test tool was installed in the drilling pipe. During the test, the formation fluid entered the drilling pipe and passed through the test tool. When the formation fluid passed through the test tool, its pressure was recorded. It was recorded in the zone of interest, for example in the Nanye 1 well the pressure was recorded in the 1544.3-4410.7 m depth. In the Pengye 1 well, the pressure was recorded at 2072-2160 m depth (in the shale formation). The pore pressure data were collected from the report of Sinopec East China Petroleum Engineering Co., Ltd, this company conducted the DSTs. The pore pressure data were collected from different wells including Shengye 1, Shengye 3, Jiaoye 194-3, Jiaoye 10-10, Longye 1, Pengye 1 (PY 1) and Nanye 1 (NY 1) wells. These wells are located southeast of the Sichuan Basin. These wells penetrated different formations composed of different lithologies including limestone, mudstone, shale and sandstone.

3.1.2. Pore pressure coefficient evaluation

After measuring the formation pore pressure (P_{re}), the pore pressure coefficient was evaluated. The pore pressure coefficient (α) is defined as the ratio of the original reservoir pore pressure to the hydrostatic column pressure. The pore pressure coefficients were calculated by using Equation (1) (Du et al., 1995).

$$\alpha = \frac{P_{re}}{P_{hydr}} \quad (1)$$

where P_{re}: formation pore pressure and P_{hydr}: hydrostatic pressure. A water density of 1.0 g/cm^3 was used in calculating hydrostatic column pressure. The pore pressure coefficient was evaluated to determine the pore pressure distribution in the formations.

In general, when the pore pressure of the formation is less than hydrostatic pressure or the pore pressure coefficient is less than 1, the formation is termed an underpressured formation. Researchers in the former Soviet Union define formations with a pore pressure coefficient less than 0.8 as ultra underpressured formations, 0.8–1.0 as underpressured formations and 1.0–1.05 as normal pressured formations (Du et al., 1995). However, EXXON company in the United States defines a formation with a pore pressure coefficient less than 0.8 as ultra underpressured formations and 0.8– 0.96 as underpressured formations (Du et al., 1995). The identification of normal to underpressured formations in this work was done based on Chinese researchers, Hao et al. (2005); Wang et al. (2020) as shown in Table 1.

3.1.3. Pore pressure depth relationship

The pore pressure distribution in the formations was evaluated based on the pore pressure depth relationship. The pore pressure increases with depth and the relationship is linear. The pore pressure data were used to plot the pressure change in different depths to evaluate the pressure distribution in the formations. The slope of the pore pressure depth plot is called the pore pressure gradient. The hydrostatic pressure gradient of many formations is 0.465 psi/ft (0.105 bar / m). The formation with a pore pressure gradient less than the hydrostatic pressure gradient is referred to as an underpressured formation. Whereas the formation with a pore pressure gradient greater than the hydrostatic pressure gradient is referred to as overpressured formation as discussed by Dahlberg (2012); Hao et al. (2012) and Lin et al. (2020)

3.2.Basin modelling

The basin modelling techniques were employed to investigate the burial and thermal maturity history of sedimentary basins. The basin modelling explains the dynamic modelling of geological processes in sedimentary basins over geological periods (Mukherjee and Kumar, 2018d). According to Amobi et al. (2019), basin modelling techniques help exploration geoscientists to simulate basin evolution, petroleum generation, expulsion, migration, and accumulation. Furthermore, the basin modelling helps to know if there were uplift, erosion, or changes in the burial depth in the formation. According to Handhal and Mahdi (2016), the temperature and pore pressure histories and their distributions can also be analysed by basin modelling.

1D modelling of burial history and thermal maturity was performed on the two wells, Pengye 1 and Nanye 1 wells, using a PetroMod 1D (v.9, 2005) simulator. PetroMod 1D is a simulator that fully integrates seismic and geological interpretation with a multidimensional simulation of thermal 3-phase fluid and petroleum migration histories in sedimentary basins. This simulator combines deposition, determination of pore pressure, compaction, analysis of heat flow, calculation of temperature, the kinetics of calibration parameters, modelling of hydrocarbon generation, adsorption and expulsion processes, fluid analysis, and lastly migration (Handhal and Mahdi, 2016). The simulator needs much information as input data. The input data in this simulator were position and thickness of formations (depth, thickness), deposition and erosion thickness, ages of deposition and erosion, lithologies, petrosystem potential elements (source rock, overburden, underburden), total organic carbon (TOC), hydrogen index (HI), and kinetics data. In modelling the basin by PetroMod 1D simulator, it was assumed that there is zero paleobathymetry, the model simulation gives valid temperature reconstruction and no significant thermal impact from igneous activities. Also, it was assumed that the sedimentary surface temperature is the same as the paleotemperature from the corresponding paleowater depth.

The input data

The Sinopec East China Petroleum Engineering Co., Ltd conducted the DST. The report of this company contains many data from the top to the bottom of the wells. So, the input data were obtained from that report. The input data obtained in that report were the names, depths, and thickness of the formations, as well as the lithologies. Also, other input data including TOC, HI and kinetics data in the zones of interest were obtained from that report.

The ages of deposition and erosion

The age of deposition and the age of erosion are very essential input data in the PetroMod 1D simulator. It is required to recognize the geological event of deposition and hiatus, as a result, one can calculate the paleo times of deposition and erosion of the layers (Hantschel and Kauerauf, 2009). In this work, the ages of erosion and deposition were obtained from literatures (Cao et al., 2020; Jing et al., 2016), these literatures contained the geological events of the SE Sichuan Basin.

Porosity determination

Compaction and porosity are decreasing as the burial depth increase. There are several methods to determine the porosity, the more accurate methods are by using open hole well logs such as sonic, neutron, and density logs. The plot of porosities versus depths was used to evaluate the compaction. Also, by knowing the initial porosity, the porosities at different depths were approximated by using Athy's equation as shown by Equation (2) (Abd Aziz et al., 2009; Mukherjee, 2018a; Mukherjee, 2018b; Mukherjee, 2018c).

$$\theta_z = \theta_o e^{-cz} \tag{2}$$

Where z: depth, θ_o: initial porosity (0.49 for Sandstone, 0.55 for Shale, 0.52 for Limestone, 0.42 for Dolomite), θ_z: porosity at depth z and c: coefficient of the curve (0.0003 for Sandstone, 0.0005 for Shale, 0.0006 for Limestone, 0.0004 for Dolomite) (Abd Aziz et al., 2009).

Eroded thickness

The eroded thickness is another important input data in the PetroMod 1D simulator. The eroded thickness was calculated from the age of erosion and age of deposition by using Equation (3) as suggested by Zhang et al. (2018).

$$T_{er} = T_0 \times \frac{A_{er}}{A_{dep}} \tag{3}$$

where T_0: original sediment thickness, T_{er}: eroded thickness, A_{er}: age of erosion and A_{dep}: age of deposition.

Sediment decompaction

The first step in sedimentation decompaction is to evaluate the original sediment thickness of the growing sedimentary fill from the basin floor and up-to-date stratigraphic boundaries in particular exposure. The original sediment thickness was evaluated from the present porosity and current thickness of the sediment by using Equation (4) (Hantschel and Kauerauf, 2009).

$$T_o = \frac{1-\theta_z}{1-\theta_o} \times T_p \tag{4}$$

Where T_p: present thickness and θ_z: current porosity.

Heat flow

The magnitude, orientation, and distribution of heat flow at the base of rocks depend on the mechanical and thermal processes of the crust and mantle (Allen and Allen, 2005). The heat flow in the basin was estimated by the mathematical model (Equation (5)) (Hantschel and Kauerauf, 2009) in-built within the simulator. The mathematical model was developed on the basis that heat transfers in the rock through conduction and radiation (by fluid in the faults) (Beardsmore et al., 2001).

$$\mathrm{Q_z} = \mathrm{k}\frac{\mathrm{dt}}{\mathrm{dz}} \tag{5}$$

Where $\mathrm{Q_z}$: vertical component of heat flow (MW m^{-1}), k: thermal conductivity (Wm^{-1} $°C^{-1}$) and $\frac{\mathrm{dt}}{\mathrm{dz}}$: geothermal gradient(°C/km).

The thermal conductivity is determined by using Equation(6) (Hantschel and Kauerauf, 2009).

$$k = k_m^{1-\theta} \times k_w^{\theta} \tag{6}$$

Where k: bulk thermal conductivity, k_w: water conductivity (0.59 Wm^{-1} $°C^{-1}$), ϕ: porosity (%) and k_m: rock matrix conductivity (1.45 for shale, 3.75 for dolomite, 2.64 for sandstone, 2.56 for limestone, 5.4 for anhydrite) (Hantschel and Kauerauf, 2009).

The heat flow was evaluated by following three procedures. Those procedures include obtaining the values of porosity, obtaining the k_m values from lithological sections of the wells, and estimating the geothermal gradient from the values of surface temperature (Ts), true depth (TD) and bottom hole temperature (BHT).

The basin modelling procedure in this work is shown in Fig. 3. First, the input data are gathered from the report of Sinopec East China Petroleum Engineering Co., Ltd, literatures, and the estimates of the mathematical models. Second, the kinetic model is selected to classify and evaluate the source rock, as well as evaluate the maturity of hydrocarbons in the formations, and then the simulator is run, and results are obtained. The third procedure involves the calibration of the model. Calibration of the model involves comparing the known or measured parameters (temperature, vitrinite reflectance and pore pressure) with the results obtained in the simulator. The calibration of the model can be done to a single selected parameter or many selected parameters. This is done to check if the selected kinetic model suits these hydrocarbon formations (source rocks). If the simulator's results are almost equal (close) to the measured parameters, then all the simulator's results will be accepted. But if the simulator's results disagree with the measured parameters, then the kinetic model will be changed until when the proper results are obtained.

So, the data collected from the exploration company report, literatures and estimates from the mathematical models were added to the simulator. Then the Sweened and Burnham (1990) _T3 model was selected to classify and evaluate the source rock as well as gas-oil-to-source correlations. Vitrinite reflectance (Ro) data were selected to calibrate the model. As shown in Fig. 4, the measured Ro (data with blue plus in the figure) was very close to the Ro estimated in the simulator by the Sweened and Burnham (1990) _T3 model (represented by the yellow line). The closeness of the measured data to the simulator's results indicated the suitability of the model in these hydrocarbon formations. Hence, all results in the model were accepted for further analysis.

3.3. Pore pressure drops caused by tectonic uplift and erosion

According to Xu et al. (2008) and Xu et al. (2010), tectonic uplift and erosion contribute to the drop of pore pressure in the formations. The tectonic uplift and erosion reduce the formation pore pressure by reducing the formation temperature and rebound of the rock porosity. A rebound of the rock porosity is the action of increasing the pore volume due to the relaxation of the rock when overburden stress is reduced. According to Xu et al. (2010), the drop in pore pressure (ΔP) which is caused by tectonic uplift and erosion can be evaluated by using Equation (7).

$$\Delta P = \left\{\frac{1}{3}\left(\frac{1+\gamma}{1-\gamma}\right)\left(\frac{\beta_r}{\beta_f+\beta_r}\right) g\rho_r\,\Delta h\right\} + \left[\frac{\alpha_f}{\beta_f+\beta_r}\Delta T\right] \quad (7)$$

Whereby γ: Poisson ratio, β_r: pore volume compressibility, β_f: liquid compression coefficient, g: acceleration due to gravity, ρ_r: density of the rock, Δh: erosion thickness, α_f: liquid expansion coefficient and ΔT: reduction in temperature. The part of Equation (7) inside the curly bracket represents the pore pressure drop due to the rebound of the rock porosity and that inside the square brackets denotes the pressure drop due to the reduction of temperature.

4. Results and Discussions

Different methods were used in identifying the normal to underpressured formations and studying the origins of underpressured formations in the SE Sichuan basin. The pore pressure coefficient evaluation and pore pressure depth plot analysis methods were used in identifying the normal to underpressured formations. Whereas, the basin evolution (showing temperature changes, pore pressure changes and maturity of organic matter), the effect of tectonic uplift and erosion and the faulting system were studied to uncover the origins of underpressured formation. The main results of this study are as follows:

4.1.Pore pressure coefficient (α)

There was a great variation of pore pressure in the Chongqing region. The average pore pressure coefficients of the wells drilled in this area were different as shown in Table 2. Pengye 1 well was having normal pore pressure, whereas other wells were overpressured. Only three wells, Nanye 1, Pengye 1, and Shengye 1 were chosen for pore pressure coefficient evaluation. Also, the two wells, Nanye 1 and Pengye 1 wells were modelled to study the origins of underpressured formations.

The Nanye 1 (NY 1) well was drilled in the Chongqing region in a place called Nanchuan. This well penetrated different formations including Jialingjiang, Feixianguan, Changxing, Longtan, Maokou, Qixia, Liangshan, Huanglong, Hanjiadian, Xiaoheba, Longmaxi, Wufeng, Linxiang, and Pagoda formations from SE Sichuan Basin (Fig. 2). The pore pressure coefficients increased with depth in the Nanye 1 well. At 1544.3-1903.6 m depth, the well-recorded pore pressure coefficients were less than 0.96. At 1903.6-2570.2 m depth, the well-pore pressure coefficients were between 0.96 and 1.06. The higher-pore pressure coefficients were recorded in the well at 3876-4410.7 m depth which reached up to 1.45 (Fig. 5).

Pengye 1 well was drilled in the southeast of the Chongqing area. The data in this well were recorded in the zone of interest (zone which contained gas), which is found at 2072-2160 m depth. The pore pressure coefficient in this well is 1.06 throughout that depth. The third well in which the pore pressure analysis was done is the Shengye 1 well. This well is found in the Nanchuan, south of the Nanye 1 well. At 1323.3-1454.6 m depth in the Shengye 1 well, the pore pressure coefficient was 1.2, at 1621.3- 1694.8 m depth it was 1.3, and at 2838.5- 2995.8 m depth was 1.1.

The normal to underpressured formations were identified based on the classification of Hao et al. (2005); Wang et al. (2020). The calculated pore pressure coefficients showed that in Nanye 1 well, the formations found at the depth between 1544.3 and 2570.2 m were having normal to underpressure, whereas others were overpressured formations. Also, the results show that the Pengye 1 well penetrated in the normal pressured formations at the depth between 2072 and 2160 m. All formations in the Shengye 1 well are overpressured formations.

4.2.Pore pressure depth plot

The variation of pore pressure in a Nanye 1 well through different formations is shown in Fig. 6. The Figure shows that in the upper formations at 1544.3-1904 m depth, the pore pressures were less than the hydrostatic pressure. This depth has three formations, the Lower Triassic Feixianguan, Upper Permian Changxing and Upper Permian Longtan Formations. At 1904-2570.2 m depth, the pore pressure was slightly higher than the hydrostatic pressure but lower than the pore pressure coefficient of 1.06. The depth has two formations, the Middle Permian Maokou and Lower Permian Qixia Formations. The pore pressure coefficients in the deep formations (Xiaoheba and Longmaxi formations) were higher than the pore pressure coefficient of 1.27.

The variation of pore pressure with depth in the Pengye 1 well is shown in Fig. 7. In this well, the data were found at 2072-2160 m depth and the pore pressure gradient was slightly higher than hydrostatic pressure but equal to the pore pressure coefficient of 1.06. All the data were recorded in the Wufeng and Longmaxi shales (a zone of interest).

The formations were classified based on pore pressure coefficient criteria as presented by Hao et al. (2005); Wang et al. (2020) and the pore pressure depth plots. In the Nanye 1 well, Lower Triassic Feixianguan, Upper Permian Changxing, Upper Permian Longtan, Middle Permian Maokou, and Lower Permian Qixia Formations were found at 1544.3-2570.2 m depth. These formations were normal to underpressured formations in the Nanchuan area. In the Pengye 1 well, the Lower Silurian Longmaxi and Upper Ordovician Wufeng Formations found at 2072-2160 m depth were termed as normal pressured formations in the SE of the Chongqing region. The stratigraphy shows the formations, which contained gas are Upper Permian Longtan, Middle Permian Maokou, Lower Silurian Longmaxi and Upper Ordovician Wufeng (Fig. 2). So, the normal to underpressured gas formations in the Nanchuan area were the Upper Permian Longtan and Middle Permian Maokou formations. The Lower Silurian Longmaxi and Upper Ordovician Wufeng formations were normal pressured gas formations in the SE of the Chongqing region.

4.3.The petroleum system

To study the changes in temperature, maturity of organic matter and pore pressure, the basins were modelled. After calibration of the model, the results were obtained as shown in Fig. 8 and Fig. 9. Fig. 8 shows the petroleum system obtained after modelling the basin by using the data from Nanye 1 well (Nanchuan area). A Petroleum system includes all the geological elements and processes that are important for oil and gas deposition. The necessary components are source rock, migration pathways, reservoir, seal and trap (Fagelnour et al., 2019). The stratigraphic column of this basin ranges from the Palaeozoic Era (Ordovician period) to recent. The basin is distributed into fourteen lithostratigraphic sections namely, Leikoupo, Jialingjiang, Feixianguan, Changxing Group, Longtan, Maokou, Qixia, Liangshan, Hanjiadian Group, Xiaoheba, Longmaxi, Wufeng, Linxiang and Pagoda units. Other formations are not shown in the figure due to the limitation of space. Fig. 9 shows the petroleum system of the SE Chongqing region modelled by the data from the Pengye 1 well. The petroleum system shows the important source rocks in the Sichuan Basin called Lower Silurian Longmaxi and Upper Ordovician Wufeng formations.

4.4. The effect of paleotemperature on the maturity of the organic matter in the SE of the Sichuan Basin

The simulation results show that the temperature of different formations was varying with time, as shown in Fig. 8. In the model, it was assumed that the formations have been formed since the Palaeozoic era when the surface temperature was 20^0C. Since that time, there were a series of temperature changes due to organic matter deposition, erosion, and tectonic uplift. Due to the subsidence and deposition of organic matter, the burial depth increased, and the temperature raised to 225^0C in the deep formations in the late Triassic. The tectonic uplift and erosion happened at the end of the Triassic (227-210 Ma) and caused the temperature of the formations to drop. In the early Cretaceous, the tectonic uplift happened again and caused the temperature to drop again. The same results are shown in Fig. 9 where the SE of the Chongqing region was modelled by using Pengye 1 well data. The subsidence of the basin caused the temperature to rise, and then the tectonic uplift and erosion reduced the temperature.

The thermal maturity of organic matter is shown in Fig. 10 by the vitrinite reflectance (Ro) for the formations of the Nanye 1 well. The figures show initially the vitrinite reflectance was 0.25%, and then it rose to 1.0% which remained constant in the whole Palaeozoic era (400 to 280 Ma). In the earlier Mesozoic (250 Ma), the vitrinite reflectance rapid increased and then increased gradually in the middle Mesozoic (150 Ma) to the earlier Cenozoic era. According to Fagelnour et al. (2019), the value of vitrinite reflectance (Ro) reflects the maturity of organic matter. For example, when Ro is equal to 0.5%, the source rock is immature, or it is in the diagenesis period. When Ro range between 0.5 to 1% the source rock is in the oil window, which is the catagenesis process. Also, when Ro ranges from 1 to 2%, the source rock is in the gas window.

The results show that the temperature affected the thermal maturity of the organic matter in the SE Sichuan Basin. As shown in Fig. 10, the temperature rise caused the rise of Ro. Due to the rise of temperature from 100 to 130^0C in the late Triassic period (240-226 Ma), the organic matter was converted to oil (Ro =1%). The continual rise of temperature caused cracking of oil to gas (The value of Ro was greater than 1%). The cracking of oil to gas caused much increase in the volume of fluid (gas) in the pore space, which increased the pore pressure. The increase in temperature and pore pressure resulted in the development of overpressured formations. The curve of temperature and vitrinite reflectance are not parallel since the rise of temperature causes an increase in vitrinite reflectance but when the temperature decreases the vitrinite reflectance remains the same (Fig. 10 and Fig. 11).

In the southeast of the Chongqing region, the rise of temperature also caused the maturity of organic matter, as shown in Fig. 11. Initially, the Lower Silurian Longmaxi and Upper Ordovician Wufeng Formations were having low temperatures and the vitrinite reflectance was small. The rise of temperature caused the maturity of organic matter to the oil window (Ro =1%) and then the cracking of oil to a gas window (Ro > 1%). The cracking of oil to gas increased fluid volume in the pore space, and then the increase in pore pressure. Due to this process, the formation became overpressured.

4.5.The origins of underpressured formations in the SE of the Sichuan Basin

The results reveal that underpressured formations in this basin originated from the overpressured formations. The overpressured formations were caused by rapid subsidence, increased temperature, and oil to gas cracking. The oil to gas cracking was the main cause of overpressure formations (Li et al., 2016). During the subsidence, the formations were buried at high depth, the increase in depth caused an increase in the vertical stress and then an increase in the pore pressure. The increase in temperature with depth caused an increase in the pore pressure. Also, the cracking of oil into gas caused an increase in the volume of gas, which increased pore pressure. But the results show that tectonic uplift and erosion occurred in the late Triassic and early Cretaceous. The tectonic uplift and erosion decreased the formations' temperature, caused pore volume resilience and enlarged a trap space, which decreased the formation pore pressure. The drop of formation pore pressures caused the development of underpressured formations, however, when the pore pressure was dropped less, other formations remained overpressured. Thus, the temperature decrease, pore volume resilience and enlarging of a trap space were the origins of underpressured formations, and these origins were influenced by tectonic uplift and erosion.

The effect of tectonic uplift which happened in 242 Ma in the Nanchuan region is shown in Fig. 12. The figure shows that in 227 Ma, Upper Permian Longtan and Middle Permian Maokou formations were overpressured formations. But the tectonic activities caused uplift of the Upper Permian Longtan and Middle Permian Maokou Formations from a depth between 4900 and 5488 m, respectively as shown in Fig. 12, a to a depth between 1904 and 2500 m as shown in Fig. 12,d. Due to the uplifting of the formations, the temperature decreased, trap space was enlarged, and pore volume increased, which resulted in a pore pressure decrease. The decrease of pore pressure resulted in the underpressured Upper Permian Longtan and Middle Permian Maokou Formations, which were initially overpressure formations. The evolution of pore pressure in these formations is seen in Fig. 12 whereby initially the formations were overpressured but when it reached 135 Ma the pore pressure was highly reduced, in 32.66 Ma the pore pressure continued to decrease and resulted in current underpressured formations as shown in Fig. 12,d.

4.6. The influence of tectonic uplift and erosion on the formation pore pressure by a mathematical model

The tectonic uplift and erosion of the rock strata cause a decrease in vertical in-situ stress. The decrease of vertical in-situ stress causes the rebound of the rock matrix. The rebound of the rock matrix causes an increase in the pore volume, which in turn decreases the pore pressure. The decrease of pore pressure due to pore rebound (ΔP_p) which is influenced by the tectonic uplift and erosion was evaluated by using the first part of Equation (7).

The modification of the second part (the part inside the square brackets) of Equation (7) is shown in Equation (8) (Hao et al., 2011).

$$\Delta P_t = \frac{\alpha_f G}{1000(\beta_f + \beta_r)} \Delta h \tag{8}$$

$$\beta_r = \frac{3(1 - 2\Upsilon)}{E} \left(\frac{4(1 - \Upsilon^2)}{3\pi(1 - 2\Upsilon)\epsilon} - 1 \right) \tag{9}$$

Whereby, Δh: erosion thickness, G: geothermal gradient that ranges from 17.7 to 33.3 °C/km in the Sichuan Basin. The formation was assumed to contain formation water, so the liquid expansion coefficient (α_f) was $5.00 \times 10^{-4} K^{-1}$ (Xu et al., 2010). The value of liquid compression coefficient (β_f) is 0.0005 MPa^{-1} and the average density of rock in these formations is 2.67 t/m^3 (Xu et al., 2010). The value of pore volume compressibility (β_r) was found by using Equation (9) as suggested by Zhang et al. (2015). The value of Poisson's ratio (Υ) ranged from 0.26 to 0.28 (Wang et al., 2017), hence the average value (0.27) was used in this study. E is the young modulus which ranges from 5-19 GPa for rock found in the SE of the Sichuan Basin and ϵ is the aspect ratio which ranges from 1.85:1 and 2.39:1 (Wang et al., 2017).

Also, the tectonic uplift and erosion raised the formations to a shallow depth, which reduced the formation temperature. The decrease of temperature in the strata reduces fluid pressure. The influence of temperature on the formation pore pressure was evaluated by using Equation (8) which is the modification of the second part of Equation (7).

The analysis of pore pressure drop considered that the formation contains only water. Table 3 shows the results of the pressure drops in different formations in the Nanchuan area. The decrease of pore pressure evaluated from the model due to a decrease in temperature varies from 29.84 MPa in the Middle Triassic Jialingjiang formation to 41.71 MPa in the Upper Permian Longtan formation. The pore pressure drops due to pore rebound vary from 3.51 MPa in the Middle Triassic Jialingjiang formation to 4.91 MPa in the Upper Permian Longtan formation. These two factors contribute to a maximum total pore pressure drop of 46.62 MPa, which results in the occurrence of underpressured formations.

The pore pressure drops evaluated by the mathematical models relate to the pore pressure evolution from the basin modelling, which is shown in Fig. 12. For example, the Upper Permian Longtan Formation had a maximum formation pore pressure of 65 MPa in 210 Ma when the formation was at a depth of 4344 m (Fig.12, b). The tectonic uplift and erosion caused the formation to rise to a depth of 1878 m and the formation pore pressure to decrease to 17 MPa (Fig.12, d). So, the pore pressure drop in the formation was 48 MPa, which is 1.38 MPa higher than that evaluated from the mathematical models. Other factors including escape of the gas through the faults and groundwater movement can be a reason for a 1.38 MPa pore pressure drop. So, these results match with Xu et al. (2008); Xu et al. (2010). These authors mentioned tectonic uplift and erosion as the factor influencing underpressured formations. Also, the results relate to the results found by Hao et al. (2011), where the total pore pressure drop due to porous rebound and temperature decrease ranged from 30.16 to 39.31 MPa. The thickness of lithology eroded in that work is less than the ones found in this work. That can be one of the reasons for the difference in pore pressure drops.

Through basin modelling and mathematical model, it was found that the underpressure in the formations is caused by pore rebounded and temperature decrease. These two factors are caused by tectonic uplift and erosion. These results agreed with other works which were conducted by Hao et al. (2011); Nelson (2012); Wang et al. (2020); Xie et al. (2003) and Duan and Wu (2020). These works stated the possible causes of underpressured formations as pore rebound and temperature reduction which were mainly caused by tectonic uplift and erosion as shown in Table 4.

4.7. Existence of faults system and their role in the underpressure development in the Nanchuan area and Southeast of Chongqing region

The SE Sichuan Basin especially at the southern margin formed when the blocks were divided due to the presence of fault systems in the region (Zhao and Coe, 1987). The other parts are the western and northern corners, as well as the eastern and western margins. Active tectonics in the Sichuan Basin developed numerous major and minor faults throughout the region (Molnar and Dayem, 2010). Among the major faults in the region are the Daba Shan, Longmen Shan, East Yangtze fold belt and Xianshuihe-Xiaojiang fault (XXF), which are found in the north, northwest, southeast and southwest, respectively (Fig. 13). The occurrence of faults in the basin was caused by different tectonic activities. The occurrences of the Longmen Shan fault in the Southern Sichuan Basin were associated with two tectonic events. The first one occurred in the Late Triassic and caused convergence between the Yangtze block and the Songpan Ganzi belt. The second event occurred in the Cenozoic and resulted in the convergence between the Tibetan plateau and the Sichuan Basin. The XXF is Sichuan's most active Cenozoic structure, causing several earthquakes with magnitudes greater than M 7.0 (Wang et al., 2014; Wang et al., 2016; WANG et al., 2008). Apart from the boundary faults, the Sichuan Basin has several active and basement faults. The active and basement faults found in the Sichuan Basin are shown in Fig. 14.

4.8. The roles of faults in the occurrence of normal and underpressured formations

In this region, faults served three purposes: partitioning the region into various compartments, each with its pore pressure system, acting as conduits for gas migration and pore pressure preservation in the basin (Fan et al., 2016). In its first role, the faults divided the basin into different regions, which are the western and northern corners and southern and eastern margins (Wang et al., 2014). These regions are separated by faults that are filled with fine materials, hence the pore pressure system differs from one region to another. The Nanye 1 well in the Nanchuan area and the Pengye 1 well in the SE of Chongqing region are separated by faults, one of them is the Hubei-Guizhou Hunan thrust fault. The existence of the faults is revealed in Fig. 15 whereby the Lower Silurian Longmaxi formation in the southeast of Chongqing region (Pengye 1 well) is found at 2072-2160 m depth and the Lower Silurian Longmaxi formation in the Nanchuan area (Nanye 1 well) is found at the depth between 4405 and 4410 m. Also, the pore pressure of these formations is different, the pore pressure coefficient of Lower Silurian Longmaxi formation in the Nanye 1 well is 1.4 whereas the pore pressure coefficient of Lower Silurian Longmaxi formation in the Pengye 1 well is 1.06. The Lower Silurian Longmaxi formations have different locations, although these formations were formed at the same time in the same condition. So, the faults in this region divided the Lower Silurian Longmaxi Formation into two compartments and then engineered the difference in the pore pressure system.

The second role played by the faults in the SE Sichuan Basin was the migration and leaking of the gas from the shale formations, as shown in Fig. 16. According to Zhang et al. (2018) during the Late Cretaceous to Palaeogene the fault-opening events occurred in the Sichuan Basin. Also, the development of the deep faults which penetrated to about 4000-6000 m depth in the SE of the Chongqing region happened (Fig. 16). The active and deep faults in the Pengshui Area caused the rapid migration of the pore fluid (gas) from the formation to the deep layers. This shale gas leaking reduced the volume of the fluid in the pore and then reduced the pore pressure. This mechanism contributed to the occurrences of underpressured formations in this region.

The third role played by the faults occurred when the active movement of faults ceased, and the faults became static. The static fault was filled with rock materials with low permeability like evaporites, siltstone and mud, and acted as a barrier to the fluid movement (Ann et al., 2005; Colin, 1987). So, static faults cut the communication between the underpressured formation and the rest formations. In limiting the communication, the formation maintained its state of low pore pressure.

4.9.The effect of the seal rocks

According to Al-Shaieb et al. (1994); Surdam et al. (1994); Whelan et al. (1994) one of the important factors in the formation of abnormal pressure in the reservoirs is the presence of seal rock. Seal rocks have low porosity and permeability that limit the communication between formations. The seal rock limits the fluids in the formation to communicate with fluids from other formations. The seal plays the role of preventing pore pressure interaction in different formations. The presence of seal rocks in the Nanchuan area in the SE Sichuan Basin helped in the conservation of pore pressure in different formations. The low pore pressures in the underpressured formations were preserved by the lateral seal rocks, labelled as seal 1 and seal 2 in Fig. 17. The data shows that the lithology of seal 1 is mainly argillaceous limestone and the porosity of this seal rock is 1%. Due to the low porosity of this layer, the fluid incurred difficulty in migrating to the upper layer, thus the formation pore pressure was conserved. The lithology of seal 2 was mainly lime mudstone with a porosity of 2.5% as reported by Sinopec East China Petroleum Engineering Co., Ltd (the exploration company). This seal limited the communication of underpressured formations with the overpressured formations.

4.10. The implication of normal to underpressured formations

The reservoir needs enough energy to push reservoir fluid to the surface. The main source of energy in the reservoir is the reservoir pore pressure. Since the identified normal to underpressured formations have low formation pore pressure, then they will face difficulty in pushing the reservoir fluid to the surface. The results will be earlier depletion of the hydrocarbon formations and low overall production of the reservoirs. All these factors will affect the economy of the production company. Hence, this report provides knowledge beneficial to reservoir and production engineers. This knowledge directs the engineers to study the methods of boosting the reservoir pore pressure or modifying the system to increase the field life and overall production.

So, the requirement of pumping effect includes the installation of a compressor in the wellbore, boosting the reservoir pore pressure by either water and/or gas flooding or reducing the separator pressure by the installation of a Low-pressure production system (LPS) as suggested by Thiruthonder and Jothy (2016) and Abd Aziz et al. (2009) are needed to overcome that difficultness.

4.11. Limitations of this study

This work is conducted only in the SE of the Sichuan Basin and only three wells were studied. Due to this limitation, we suggest researchers to study the underpressured formations and their origins in other basins in the world such as the Persian Gulf, West Siberia, Volga-Ural, Timan-Barents Sea, Mexican and Mediterranean Basins. But also, more data from many wells and seismic data have to be considered.

5. Conclusions

The Sichuan Basin has great potential for natural gas, which is estimated to be 626 trillion cubic feet (Tcf) of technically recoverable shale gas resources. Many fields in the Sichuan Basin are termed "overpressured formations", but few wells and E&P of shale gas in the SE Sichuan Basin show the availability of normal pressured and underpressured formations. To identify normal and underpressured formations in the SE of the Sichuan Basin, we used the pore pressure estimation method. Whereas to analyse their origins, we use basin modelling, investigating the effect of tectonic uplift and erosion (by mathematical model), and also studying the effect of the fault system. From this work, the following conclusions were drawn:

1. This study identifies the Upper Permian Longtan and Middle Permian Maokou Formations in the Nanchuan area in the SE Sichuan Basin, as normal to underpressured formations with significant natural gas potential. Also, the study identifies the Lower Silurian Longmaxi and Upper Ordovician Wufeng Formations in the Pengshui Area, SE of the Chongqing region, as normal pressured formations with significant shale gas potential.
2. The main origins of underpressured formations identified in this work were temperature decrease, the rebound of the rock porosity and migration of the gas from the formation through the faults. The pore pressure drops contributed by temperature decrease and pore rebound were up to 41.71 and 3.51 MPa, respectively. These origins were mainly influenced by the tectonic uplift and erosion.

3. Another factor that played a greater role in the formation of underpressured formations was the presence of a faults system in the southeast margin of the Sichuan Basin. The faults served three roles: partitioning the region into various compartments, each with its pore pressure system, acting as conduits for gas migration and leaking and decrease in reservoir pore pressure. The fault seals preserved the developed low pore pressure in the formations. Also, the lateral rocks, above and below the underpressured formations, were having very tight properties of permeability and porosity (porosity was less or equal to 2.5%). So, the lateral rocks acted as a barrier to fluid movement, which resulted in low pore pressure preservation.

Acknowledgements

The authors would like to acknowledge the financial support of the key project of the National Natural Science Foundation of China (No. 42130803). Also, special thanks are given to the China Scholarship Council (CSC No.:2019GBJ002427) for sponsoring the first author to study and conduct research at the China University of Geosciences at Wuhan. Furthermore, the authors would like to thank Soumyajit Mukherjee (IIT Bombay) who provided a detailed review.

References

Abd Aziz, M. B., Ibrahim, Z. B., Mohamed, N., & Latif, N. (2009). *Low Pressure System: A Production Enhancement Initiative by PETRONAS.* Paper presented at the Asia Pacific Oil and Gas Conference & Exhibition.

Al-Shaieb, Z., Puckette, J. O., Abdalla, A. A., Tigert, V., & Ortoleva, P. J. (1994). The banded character of pressure seals.

Allen, P., & Allen, J. (2005). Basin analysis Principles and Applications. In: Blackwell Scientific Publications, Oxford.

Amobi, J. O., Okogbue, C. O., Mode, A. W., Ofoma, A. E., Dim, C. I. P., & Okwara, I. C. (2019). Regional 1D hydrocarbon maturation modelling of the Cenomanian-Turonian Lokpanta Shale, southern Benue Trough, Nigeria: Implications for the origin of Niger Delta deep sea oils. *Journal of Earth System Science, 128*(7). doi:10.1007/s12040-019-1192-8

Andreotti, B., Forterre, Y , & Pouliquen, O. (2013). Granular media: between fluid and solid. *Cambridge University Press*.

Ann, M., Yafes, A., William, E., & Craig, S. (2005). The rate of pressure dissipation from abnormally pressured compartments. *AAPG bulletin, 89*(1), 61-80.

Barker, C. (1972). Aquathermal pressuring—role of temperature in development of abnormal-pressure zones. *AAPG bulletin, 56*(10), 2068-2071.

Beardsmore, G. R., Cull, J. P., & Cull, J. P. (2001). *Crustal heat flow: a guide to measurement and modelling*: Cambridge university press.

Bradley, J. S. (1975). Abnormal formation pressure. *AAPG bulletin, 59*(6), 957-973.

Cao, C., Li, L., Liu, Y., Du, L., Li, Z., & He, J. (2020). Factors Affecting Shale Gas Chemistry and Stable Isotope and Noble Gas Isotope Composition and Distribution: A Case Study of Lower Silurian Longmaxi Shale Gas, Sichuan Basin. *Energies, 13*(22), 5981.

Colin, B. (1987). Development of abnormal and subnormal pressures in reservoirs containing bacterially generated gas. *AAPG bulletin, 71*(11), 1404-1413.

Dahlberg, E. C. (2012). *Applied hydrodynamics in petroleum exploration*: Springer Science & Business Media.

Dasgupta, T., & Mukherjee, S. (2020). *Sediment compaction and applications in petroleum geoscience*: Springer.

Dickey, P. A., & Cox, W. C. (1977). Oil and gas in reservoirs with subnormal pressures. *AAPG bulletin, 61*(12), 2134-2142.

Du, X., Zheng, H., & Jiao, X. (1995). Abnormal pressure and hydrocarbon accumulation. *Earth Science Frontiers, 2*(3-4), 137-148.

Duan, Y., & Wu, Y. (2020). Distribution and formation of Mesozoic low permeability underpressured oil reservoirs in the Ordos Basin, China. *Journal of Petroleum Science and Engineering, 187*, 106755.

Fagelnour, M., Gamil, I., El Toukhy, M., Gharieb, A., & Saad, H. (2019). *Source Rock Potentiality, Basin Modeling, and Oil to Source Correlation in Northern Shushan Basin, Western Desert, Egypt.* Paper presented at the Offshore Mediterranean Conference and Exhibition.

Fagelnour, M., Gamil, I., El Toukhy, M., Gharieb, A., & Saad, H. (2019). *Source Rock Potentiality, Basin Modeling, and Oil to Source Correlation in Northern*

Shushan Basin, Western Desert, Egypt. Paper presented at the Offshore Mediterranean Conference and Exhibition, Ravenna, Italy. https://doi.org/

Fan, C., Wang, Z., Wang, A., Fu, S., Wang, L., Zhang, Y., . . . Zhang, X. (2016). Identification and calculation of transfer overpressure in the northern Qaidam Basin, northwest China. *AAPG bulletin, 100*(1), 23-39.

Feng, Z., Peng, Y., Jin, Z., & Bao, Z. (2003). Lithofacies palaeogeography of the early Ordovician in China. *Journal of Palaeogeography, 5*(1), 2-14.

Guo, L., Jiang, Z., Zhang, J., & Li, Y. (2011). Paleoenvironment of Lower Silurian black shale and its significance to the potential of shale gas, southeast of Chongqing, China. *Energy Exploration & Exploitation, 29*(5), 597-616.

Guo, X. (2019). Major factors controlling the shale gas accumulations in Wufeng-Longmaxi Formation of the Pingqiao Shale Gas Field in Fuling Area, Sichuan Basin, China. *Journal of Natural Gas Geoscience, 4*(3), 129-138.

Hailong, X., Guoqi, W., Chengzao, J., Wei, Y., Tianwei, Z., Wuren, X., . . . Beiwei, L. (2012). Tectonic evolution of the Leshan-Longnüsi paleo-uplift and its control on gas accumulation in the Sinian strata. *Petroleum Exploration and development, 39*(4), 436-446.

Handhal, A. M., & Mahdi, M. M. (2016). Basin modeling analysis and organic maturation for selected wells from different oil fields, Southern Iraq. *Modeling Earth Systems and Environment, 2*(4), 1-14.

Hantschel, T., & Kauerauf, A. I. (2009). *Fundamentals of basin and petroleum systems modeling*: Springer Science & Business Media.

Hao, F., Jin, Z., & Zou, H. (2005). Kinetics of hydrocarbon generation and mechanisms of petroleum accumulation in overpressured basins. In: Beijing, China, Science Press.

Hao, X., Tang, D., Zhang, J., Yin, W., & Chen, X. (2011). Formation mechanism of underpressured reservoir in Huatugou oilfield of Qaidam basin. *Journal of Earth Science, 22*(5), 632.

Hao, X., Tang, D., Zhang, J., Yin, W., & Chen, X. (2011). Formation mechanism of underpressured reservoir in Huatugou oilfield of Qaidam basin. *Journal of Earth Science, 22*(5), 632-639.

Hao, X., Zhang, J., Dazhen, T., Ming, L., ZHANG, W., & Wenji, L. (2012). Controlling factors of underpressure reservoirs in the Sulige gas field, Ordos Basin. *Petroleum Exploration and development, 39*(1), 70-74.

Hong, F., Jiang, L., Zhuo, Q., Zhang, F., Lu, X., Ma, X., & Hao, J. (2018). Types of abnormal high-pressure gas reservoir in foreland basins of China. *Journal of Natural Gas Geoscience, 3*(4), 191-201.

Hunt, J. M. (1990). Generation and migration of petroleum from abnormally pressured fluid compartments. *AAPG bulletin, 74*(1), 1-12.

Jiang, S., Peng, Y., Gao, B., Zhang, J., Cai, D., Xue, G., . . . Dahdah, N. (2016). Geology and shale gas resource potentials in the Sichuan Basin, China. *Energy Exploration & Exploitation, 34*(5), 689-710.

Jiang, S., Tang, X., Long, S., McLennan, J., Jiang, Z., Jiang, Z., . . . Shi, X. (2017). Reservoir quality, gas accumulation and completion quality assessment of Silurian Longmaxi marine shale gas play in the Sichuan Basin, China. *Journal of Natural Gas Science and Engineering, 39,* 203-215.

Jing, T., Zhang, J., Xu, S., Liu, Z., & Han, S. (2016). Critical geological characteristics and gas-bearing controlling factors in Longmaxi shales in southeastern Chongqing, China. *Energy Exploration & Exploitation*, *34*(1), 42-60.

Korsch, R., Huazhao, M., Zhaocai, S., & Gorter, J. (1991). The Sichuan basin, southwest China: a late proterozoic (Sinian) petroleum province. *Precambrian Research*, *54*(1), 45-63.

Law, B. E., & Dicknson, W. (1985). Conceptual model for origin of abnormally pressured gas accumulations in low-permeability reservoirs. *AAPG bulletin, 69*(8), 1295-1304.

Lei, X., Su, J., & Wang, Z. (2020). Growing seismicity in the Sichuan Basin and its association with industrial activities. *Science China Earth Sciences*, 1-28.

Lei, X., Wang, Z., & Su, J. (2019). The December 2018 ML 5.7 and January 2019 ML 5.3 earthquakes in South Sichuan basin induced by shale gas hydraulic fracturing. *Seismological Research Letters, 90*(3), 1099-1110.

Li, S., Yuan, Y., Sun, W., Sun, D., & Jin, Z. (2016). Formation and destruction mechanism as well as major controlling factors of the Silurian shale gas overpressure in the Sichuan Basin, China. *Journal of Natural Gas Geoscience, 1*(4), 287-294.

Lin, B., & Wang, T. (2012). Forecasting natural gas supply in China: production peak and import trends. *Energy policy, 49*, 225-233.

Lin, X., Zeng, J., Wang, J., & Huang, M. (2020). Natural Gas Reservoir Characteristics and Non-Darcy Flow in Low-Permeability Sandstone Reservoir of Sulige Gas Field, Ordos Basin. *Energies, 13*(7), 1774.

Liu, S., F,, Ma, Y., S, , & Wang, G., Z,. (2014). Formation Process and Mechanism of the Sinian-Silurian Natural

Gas Reservoirs in the Sichuan Basin. *Beijing: Science Press (in Chinese)*.

Liu, X., & Xie, X. (2002). The characteristics of under pressure system and mechanism on origin in Dongying depression. *Oil Gas Geol (in Chinese), 23*(1), 66-70.

Liu, Y., Qiu, N., Xie, Z., Yao, Q., & Zhu, C. (2016). Overpressure compartments in the central paleo-uplift, Sichuan Basin, southwest China. *AAPG Bulletin, 100*(5), 867-888.

Liu, Y., Qiu, N., Yao, Q., Chang, J., & Xie, Z. (2016). Distribution, origin and evolution of the Upper Triassic overpressures in the central portion of the Sichuan Basin, SW China. *Journal of Petroleum Science and Engineering, 146*, 1116-1129.

Liu, Y., Qiu, N., Yao, Q., & Zhu, C. (2017). The impact of temperature on overpressure unloading in the central Sichuan Basin, southwest China. *Journal of Petroleum Science and Engineering, 156*, 142-151.

Molnar, P., & Dayem, K. E. (2010). Major intracontinental strike-slip faults and contrasts in lithospheric strength. *Geosphere, 6*(4), 444-467.

Mukherjee, S. (2018a). Moment of inertia for rock blocks subject to bookshelf faulting with geologically plausible density distributions. *Journal of Earth System Science, 127*(6), 1-7.

Mukherjee, S. (2018b). Locating center of gravity in geological contexts. *International Journal of Earth Sciences, 107*(5), 1935-1939.

Mukherjee, S. (2018c). Locating center of pressure in 2D geological situations. *J Indian Geophys Union, 22*(1), 49-51.

Mukherjee, S., & Kumar, N. (2018d). A first-order model for temperature rise for uniform and differential compression of sediments in basins. *International Journal of Earth Sciences, 107*(8), 2999-3004.

Nedderman, R. M. (2005). Statics and kinematics of granular materials. *Cambridge University Press*.

Nelson, P. (2012). Overpressure, Normal Pressure, and Underpressure and Their Coexistence in the Anadarko Basin*. *AAPG*.

Nelson, P. H. (2012). Overpressure, Normal Pressure, and Underpressure

and Their Coexistence in the Anadarko Basin*.

Neuzil, C., & Pollock, D. (1983). Erosional unloading and fluid pressures in hydraulically" tight" rocks. *The Journal of Geology, 91*(2), 179-193.

Nie, H., Jin, Z., Ma, X., Liu, Z., Lin, T., & Yang, Z. (2017). Dispositional characteristics of Ordovician Wufeng formation and Silurian Longmaxi formation in Sichuan Basin and its adjacent areas. *Petroleum Research, 2*(3), 233-246.

Qi, X., Hu, Q., Yi, X., & Zhang, S. (2015). Shale gas exploration prospect of Lower Cambrian Wangyinpu formation in Xiuwu Basin. *China Mining Magazine, 24*(10), 102-107.

Serebryakov, V., Robertson Jr, J., & Chilingarian, G. (2002). *Origin and prediction of abnormal formation pressures*: Gulf Professional Publishing.

Shu-Gen, L., Bin, D., & Yong, Z. (2016). Unique geologic features of burial and superimposition of the Lower Paleozoic shale gas across the Sichuan basin and its periphery. *Earth Science Frontiers, 23*(1), 11.

Shugen, L., Chuan, Q., Wei, S., Guozhi, W., Guosheng, X., Haifeng, Y., . . . ZhiJing, Z. (2012). The coupling formation process of four centers of hydrocarbon in Sinian Dengying Formation of Sichuan Basin. *Acta Petrologica Sinica, 28*(3), 879-888.

Sorenson, R. P. (2005). A dynamic model for the Permian Panhandle and Hugoton fields, western Anadarko basin. *AAPG bulletin, 89*(7), 921-938.

Surdam, R. C., Jiao, Z. S., & Martinsen, R. S. (1994). The regional pressure regime in Cretaceous sandstones and shales in the Powder River Basin.

Thiruthonder, H., & Jothy, A. (2016). *Low Pressure Production Unit LPPU*. Paper presented at the Offshore Technology Conference Asia.

Wang, E., Meng, K., Su, Z., Meng, Q., Chu, J. J., Chen, Z., . . . Liang, X. (2014). Block rotation: Tectonic response of the Sichuan basin to the southeastward growth of the Tibetan Plateau along the Xianshuihe-Xiaojiang fault. *Tectonics, 33*(5), 686-718.

Wang, F. (2003). Tectonic-lithofacies palaeogeography of the Silurian in Sichuan-Yunnan-Guizhou-Guangxi region. *Journal of Palaeogeography, 5*, 180-186.

Wang, G., Ju, Y., & Han, K. (2015). Early Paleozoic shale properties and gas potential evaluation in Xiuwu Basin, western Lower Yangtze Platform. *Journal of Natural Gas Science and Engineering, 22*, 489-497.

Wang, M., Hubbard, J., Plesch, A., Shaw, J. H., & Wang, L. (2016). Three-dimensional seismic velocity structure in the Sichuan basin, China. *Journal of Geophysical Research: Solid Earth, 121*(2), 1007-1022.

Wang, P. (2020). Shale gas potential in China-a production forcast for the Wufeng Longmaxi formation and implications for future development.

Wang, Q., Chen, D., Wang, F., Gao, X., Zou, Y., Tian, Z., . . . Yao, D. (2021). Origin and distribution of an under-pressured tight sandstone reservoir: The Shaximiao Formation, Central Sichuan Basin. *Marine and Petroleum Geology, 132*, 105208.

Wang, Q., Chen, D., Wang, F., Li, J., Liao, W., Wang, Z., . . . Shi, X. (2020). Underpressure characteristics and origins in the deep strata of rift basins: a case study of the Huimin Depression, Bohai Bay Basin, China. *Geological Journal, 55*(6), 4079-4096.

Wang, T., Zhang, D., Ji, Q., & Shi, X. (2020). Market reforms and determinants of import natural gas prices in China. *Energy, 196*, 117105.

Wang, W., Wu, J., Fang, L., Lai, G., & Cai, Y. (2017). Crustal thickness and Poisson's ratio in southwest China based on data from dense seismic arrays. *Journal of Geophysical Research: Solid Earth, 122*(9), 7219-7235.

Wang, X., & Zhu, Y. (2020). The Genetic Mechanism and Evolution Process of Overpressure in the Upper Ordovician–Lower Silurian Black Shale Formation in the Southern Sichuan Basin. *Minerals, 10*(3), 238.

WANG, Z.-c., ZHAO, W.-z., LI, Z.-y., JIANG, X.-f., & Jun, L. (2008). Role of basement faults in gas accumulation of Xujiahe Formation, Sichuan Basin. *Petroleum Exploration and development, 35*(5), 541-547.

Whelan, J. K., Buxton, L., & Cathles III, L. M. (1994). Pressure Seals--Interactions with Organic Matter, Experimental Observations, and Relation to a.

Wo, Y.-j., Zhou, Y., & Xiao, K.-h. (2007). The burial history and models for hydrocarbon generation and evolution in the marine strata in southern China. *Sedimentary Geology and Tethyan Geology, 27*(3), 100.

Xie, X., Jiao, J. J., Tang, Z., & Zheng, C. (2003). Evolution of abnormally low pressure and its implications for the hydrocarbon system in the southeast uplift zone of Songliao basin, China. *AAPG bulletin, 87*(1), 99-119.

Xie, Z., Yang, W., Gao, J., Jin, H., Xie, W.-r., & Shi, Z.-s. (2009). The characteristics of fluid inclusion of Xujiahe Formation reservoirs in central-south Sichuan Basin and its pool-forming significance. *Bulletin of Mineralogy, Petrology and Geochemistry (in Chinese), 28*(1), 48-52.

Xu, H., Tang, D., Zhang, J., & YIN, W. (2008). Mechanism of water table affecting reservoir pressure. *Coal Geology & Exploration, 36*(5), 31-33.

Xu, H., Zhang, J., Jia, C., Tang, D., & Yin, W. (2010). Influence of tectonic uplift-erosion on formation pressure. *Petroleum Science, 7*(4), 477-484.

Xu, Q., Qiu, N., Liu, W., Shen, A., Wang, X., & Zhang, G. (2018). Characteristics of the temperature–pressure field evolution of Middle Permian system in the northwest of Sichuan Basin. *Energy Exploration & Exploitation, 36*(4), 705-726.

Yang, J., Gao, S., & Wang, Z. (2003). Pore pressure characteristics and petroleum migration in the Upper Triassic Formation in the central-southern of the Sichuan Basin. *Gas Exploration and Development (in Chinese), 26*(2), 6-11.

Yang, R., He, S., Li, T., Yang, X., & Hu, Q. (2016). Origin of over-pressure in clastic rocks in Yuanba area, northeast Sichuan Basin, China. *Journal of Natural Gas Science and Engineering, 30*, 90-105.

Yi-Feng, L., Lun-Ju, Z., Nan-Sheng, Q., Jing-Kun, J., & Qing, C. (2015). The Effect of Temperature on the Overpressure Distribution and Formation in the Central

Paleo-Uplift of the Sichuan Basin. *Chinese Journal of Geophysics, 58*(4), 340-351.

Zeng, L. (2010). Microfracturing in the Upper Triassic Sichuan Basin tight-gas sandstones: Tectonic, overpressure, and diagenetic origins. *AAPG Bulletin, 94*(12), 1811-1825.

Zhang, K., Jiang, Z., Xie, X., Gao, Z., Liu, T., Yin, L., . . . Wu, Y. (2018). Lateral percolation and its effect on shale gas accumulation on the basis of complex tectonic background. *Geofluids, 2018*.

Zhang, R., Ning, Z., Yang, F., & Zhao, H. (2015). *Evaluation of petrophysical and mechanical features for shale gas reservoirs in South Sichuan Basin, China.* Paper presented at the EUROPEC 2015.

Zhao, L., Zhou, P., Lou, Y., Zhao, Y., Liu, W., Liao, Z., & Xia, P. (2021). Geochemical Characteristics and Sedimentary Environment of the Upper Permian Longtan Coal Series Shale in Western Guizhou Province, South China. *Geofluids, 2021*.

Zhao, X., & Coe, R. S. (1987). Palaeomagnetic constraints on the collision and rotation of North and South China. *Nature, 327*(6118), 141-144.

Zhili, L. (1998). NEW RECOGNITION OF BASEMENT IN SICHUAN BASIN [J]. *Journal of Chengdu University of Technology, 2*.

Table 1: The classification of formations based on pore pressure coefficient (Hao et al., 2005; Wang et al., 2020)

Pressure coefficient (α)	Classification
<0.8	Strong underpressure
0.8–0.96	Underpressure
0.96–1.06	Normal pressure
1.06–1.27	Weak overpressure
1.27–1.73	Overpressure
>1.73	Strong overpressure

Table 2: Average pore pressure coefficients for different wells in SE of Sichuan Basin

Wells	**Average pore pressure coefficients**
Pengye 1	1
Shengye 1	1.2
Nanye 1	1.37
Jiaoye 194-3	1.35
Longye 1	1.3
Shengye 3	1.2
Jiaoye 10-10	1.2

Table 3: The pore pressure drops caused by the decrease in temperature and rebound of the rock porosity obtained from the mathematical model in the Nanye 1 well

Formations	The erosion thickness (m)	Pore pressure drops due to temperature (MPa)	Pore pressure drops due to the rebound of the rock porosity (MPa)	Total pore pressure drops (MPa)
Jialingjiang Formation	1917	29.84	3.51	33.35
Feixianguan Formation	2459	38.27	4.51	42.78
Changxing Group	2395	37.28	4.39	41.67
Longtan Formation	2680	41.71	4.91	46.62
Maokou Formation	2400	37.35	4.40	41.75
Qixia Formation	2666	41.50	4.89	46.38
Hanjiadian Group	2480	38.60	4.54	43.14
Xiaoheba Formation	2347	36.53	4.30	40.83
Longmaxi Formation	2655	41.32	4.87	46.19

Table 4: Findings of the main factors contributing to underpressured formations in some fields and Basins

Underpressured Basins/field/formation	Methods used	Findings on the origins of underpressured formations	Citation
Huatugou Oilfield of Qaidam Basin	Mathematical models and extensive study of literature	Tectonic uplift and erosion caused pore rebound and temperature decrease. The impact of these factors is a total pore pressure drop of 30.16 to 39.31 MPa.	Hao et al. (2011)
Huimin Depression, Bohai Bay Basin, China	Pressure measurement, well logs response, seismic data evaluation, mathematical models and basin modelling	The rock dilation and temperature reduction caused pressure reductions of 3–4 and 1–3 MPa, respectively.	Wang et al. (2020)
Anadarko Basin	Basin modelling	Uplift and erosion during the Late Tertiary caused underpressured formations in the Anadarko Basin.	Nelson (2012)
Sulige gas field, Ordos Basin	Mathematical models and basin modelling	The pore rebound and temperature decrease caused by intense tectonic uplift after the late period of Early Cretaceous, caused the pore pressure of the Sulige gas field to reduce by 0.673 MPa and 23.08% of the original strata pressure, respectively.	Hao et al. (2012)
Songliao basin, China	Numerical simulation of pressure evolution.	Uplift and erosion, as well as reduction of geothermal gradients. These factors lead to significantly underpressured at about 50–80% of hydrostatic pressure.	Xie et al. (2003)
Ordos Basin, China	Mathematical models and basin modelling	Strong uplift for a long time caused increases in the eroded stratum thickness and temperature decrease in the reservoirs. These factors caused the formation pressure to be reduced to a pressure coefficient of 0.63 to 0.86.	Duan and Wu (2020)

Sinian–Silurian natural gas reservoirs in the Sichuan Basin	Basin modelling and mathematical models.	The tectonic uplift and erosion decrease the temperature and the decrease in temperature causes the decrease in pore pressure (2.3% of the pressure is decreased for every 10^0C decrease in temperature).	Liu et al. (2014)

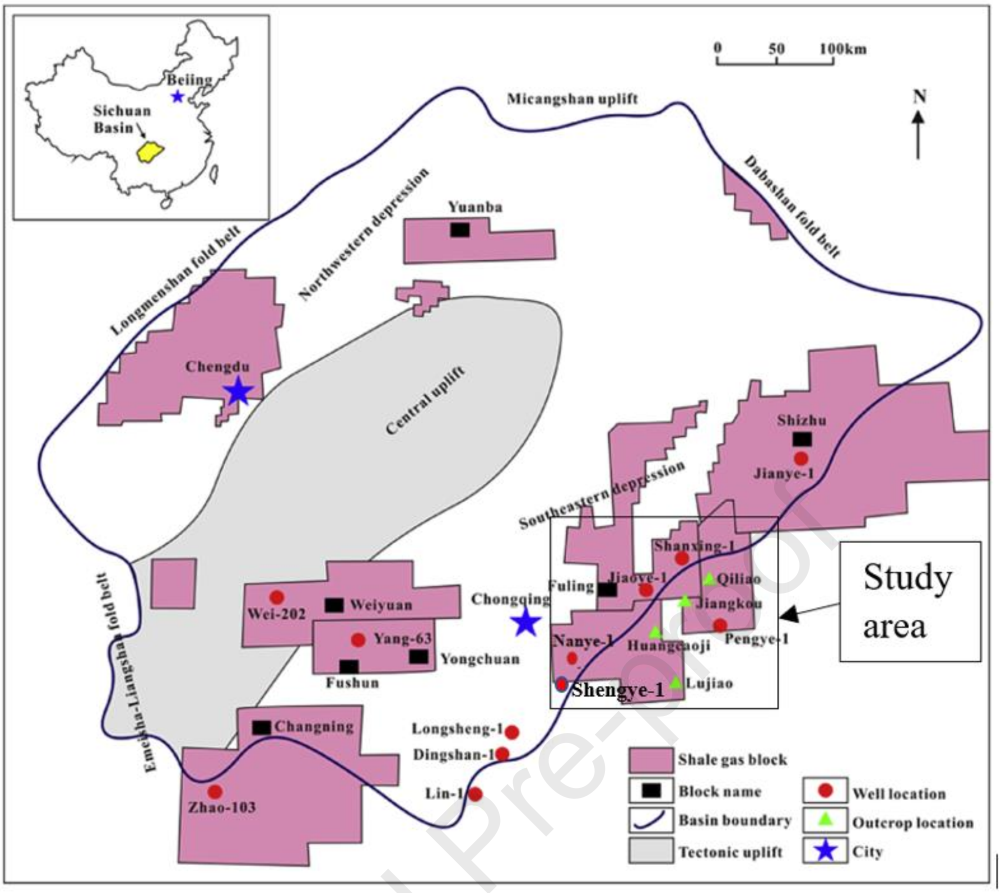

Fig. 1: The location of the Sichuan Basin, its wells, and shale blocks (Modified from Guo (2019); Jiang et al. (2017))

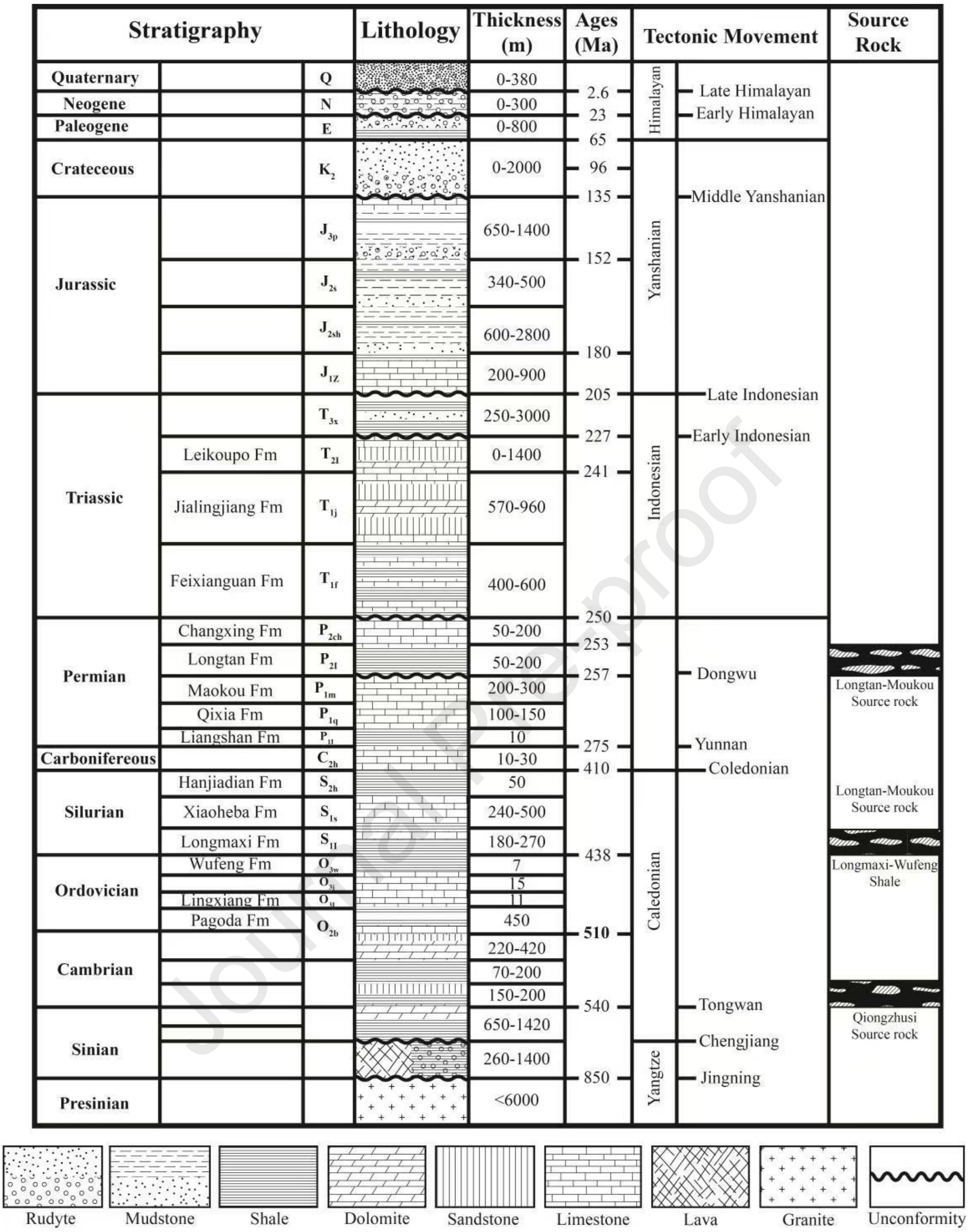

Fig. 2: The stratigraphy of the SE Sichuan basin (Modified from (Cao et al., 2020)

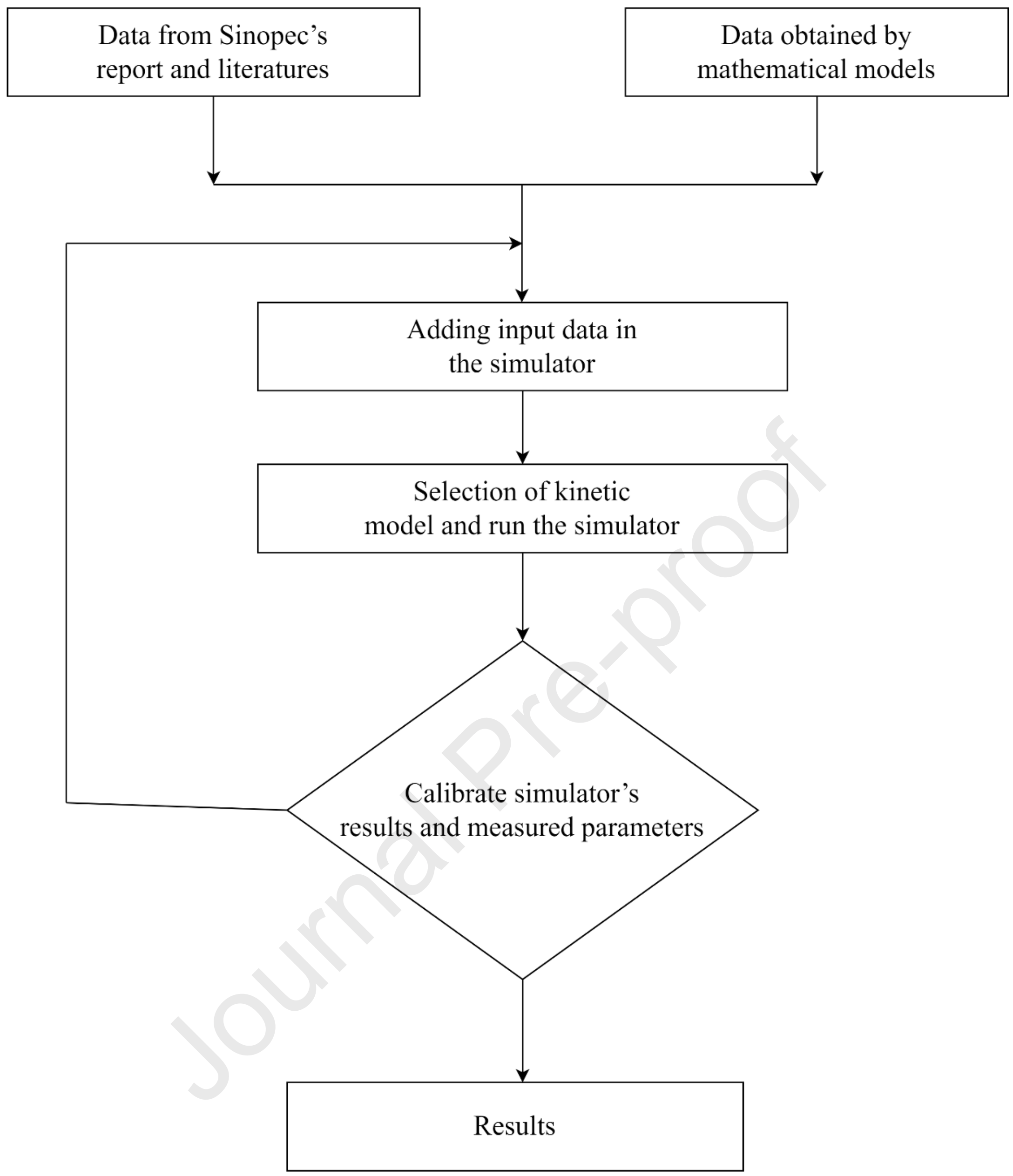

Fig. 3: The procedures followed in modelling the SE Sichuan Basin by PetroMod 1D simulator

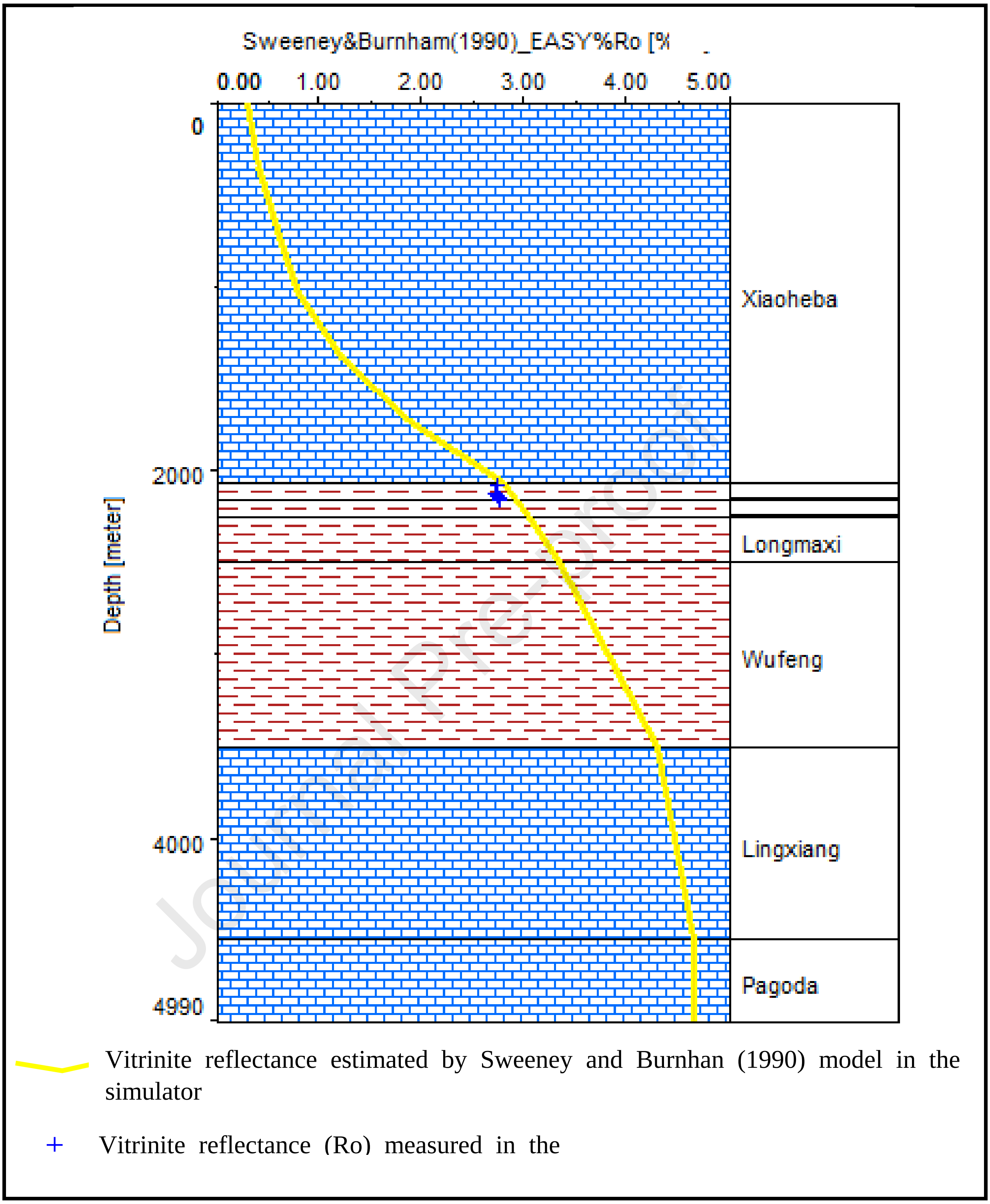

Fig. 4: The calibration of the model by using vitrinite reflectance (Ro), the Ro measured in the Pengye 1 well (blue plus) is very close to the line of Ro obtained from the simulator. The Ro in the well was measured at 2081-2153.42 m depth in the source rocks

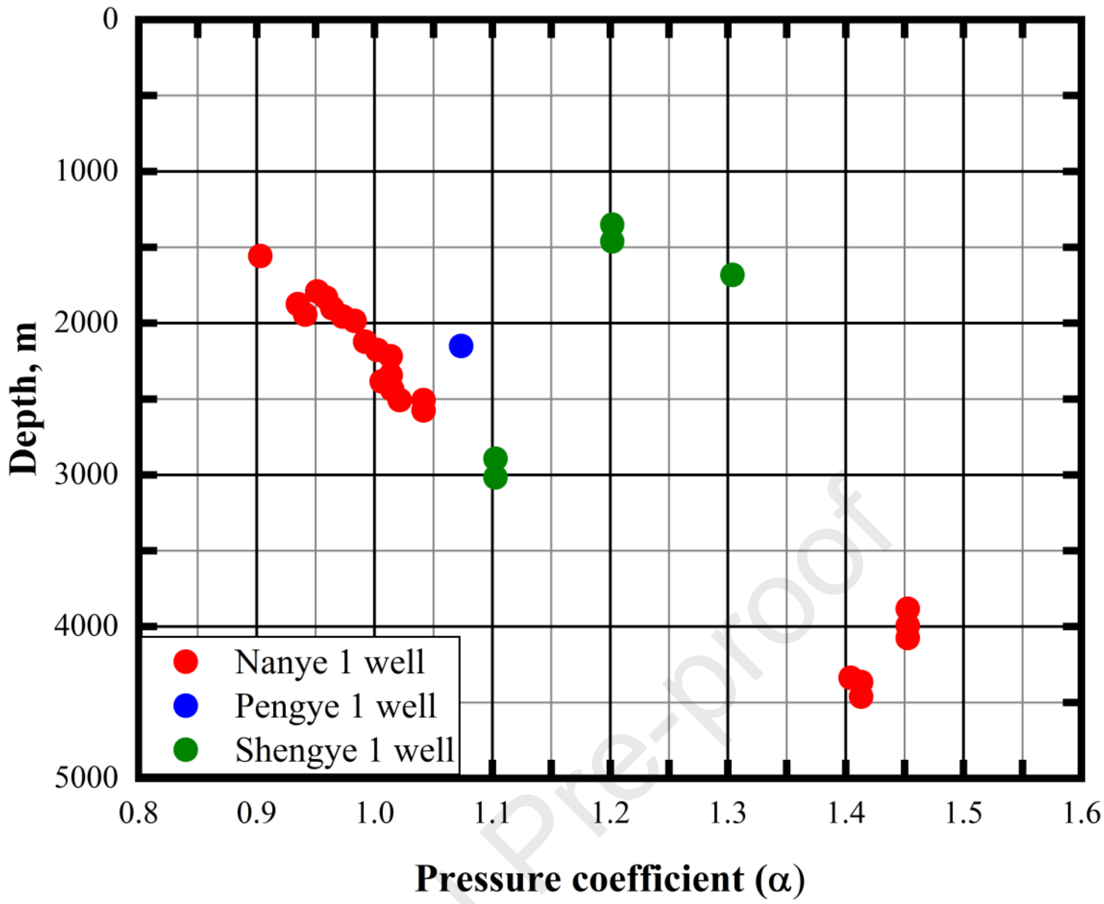

Fig. 5: Distribution of pore pressure coefficient (α) for Shenye 1, Nanye 1 l and Pengye 1 wells found in the Chongqing region in the SE Sichuan basin

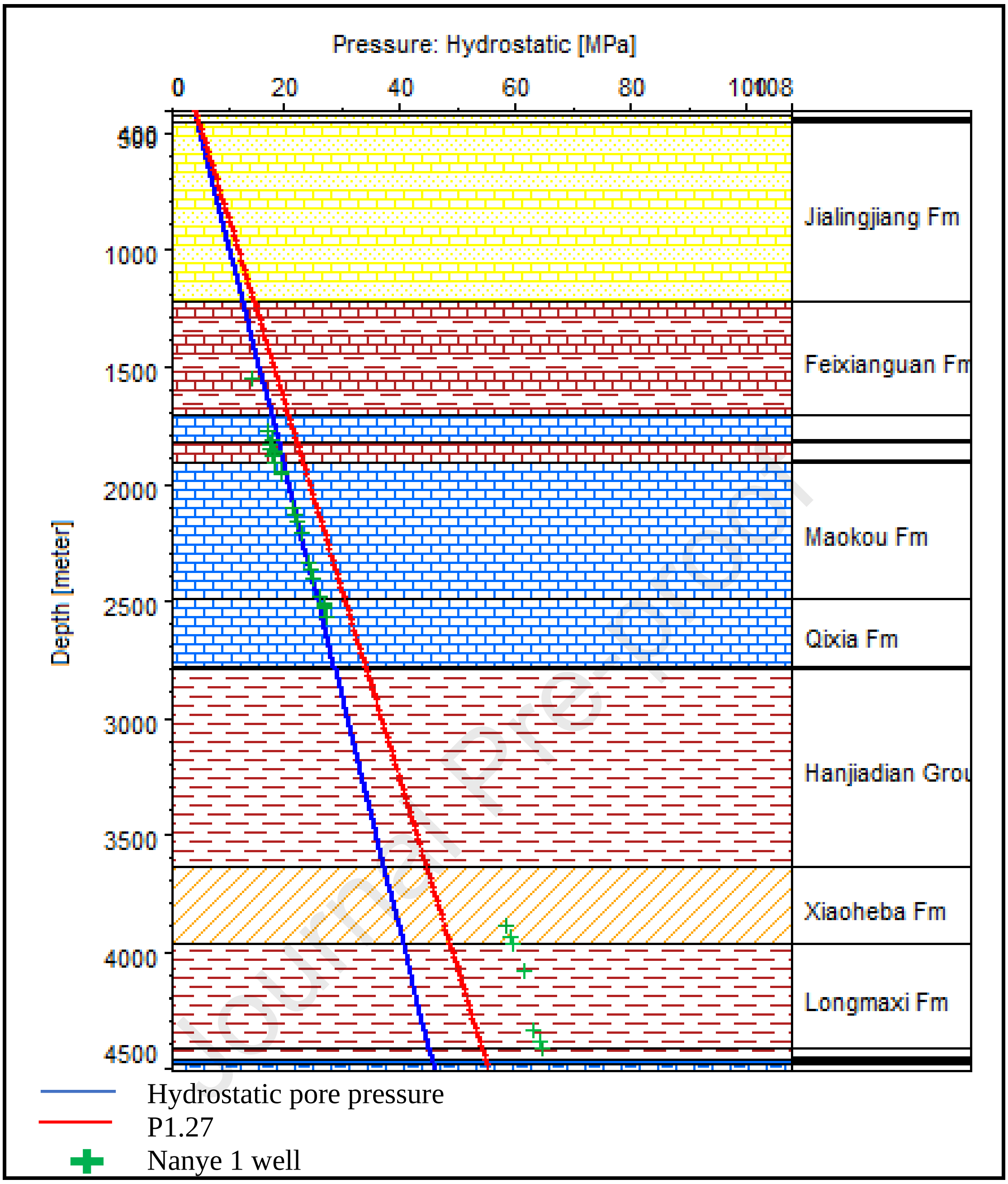

Fig. 6: The pore pressure depth plot showing the pore pressure of Nanye 1 well (represented by a green cross) when compared to the hydrostatic pore pressure (blue line) and line with a pore pressure coefficient of 1.27 (red line)

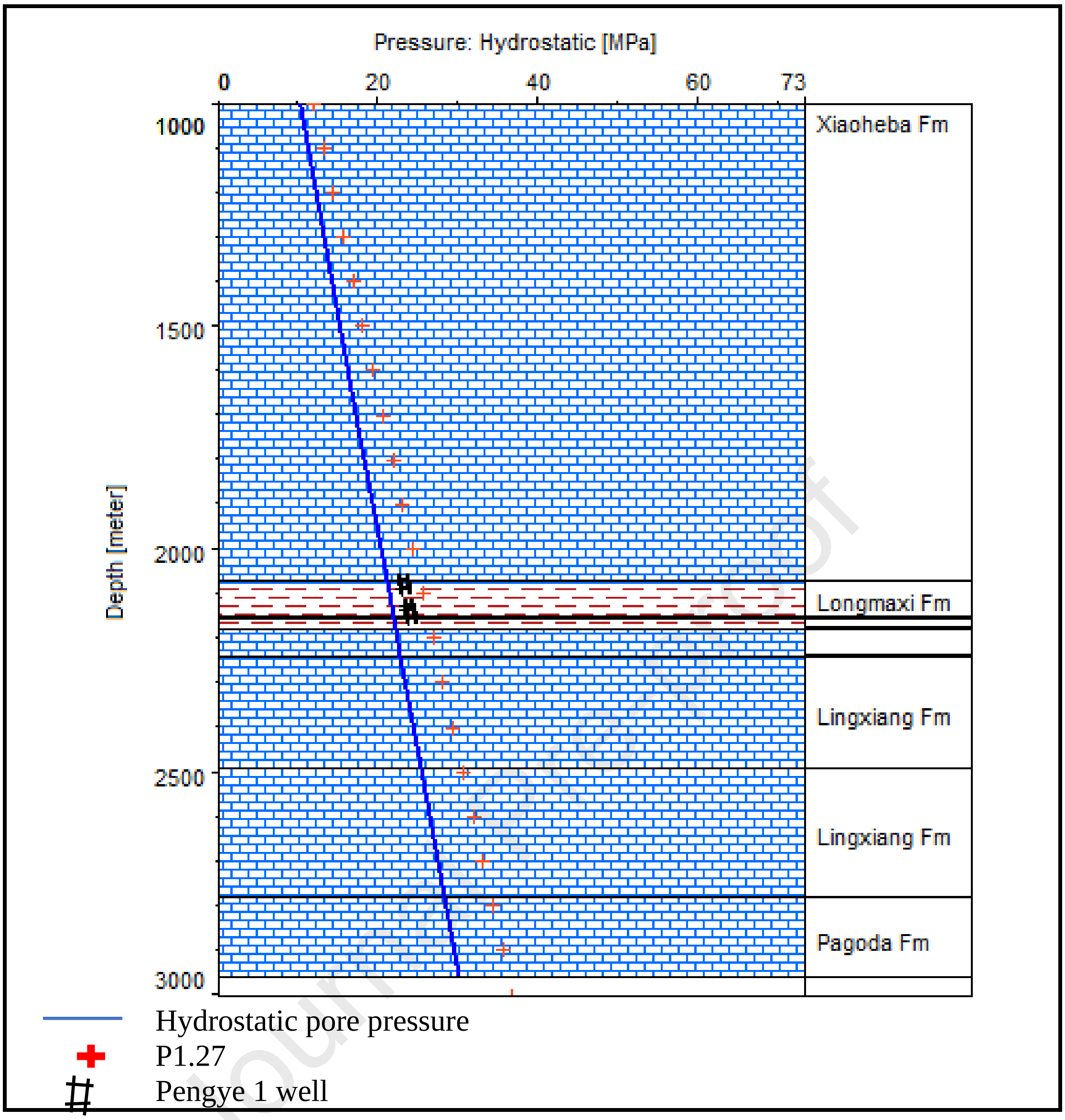

Fig. 7: The variation of pore pressure with depth in the Pengye 1 well, the black markers represent the pore pressure in the Pengye 1 well at a depth between 2072 and 2160 m (Zone of interest), the blue line represents the hydrostatic pore pressure and red cross represent the region with pore pressure coefficient of 1.27.

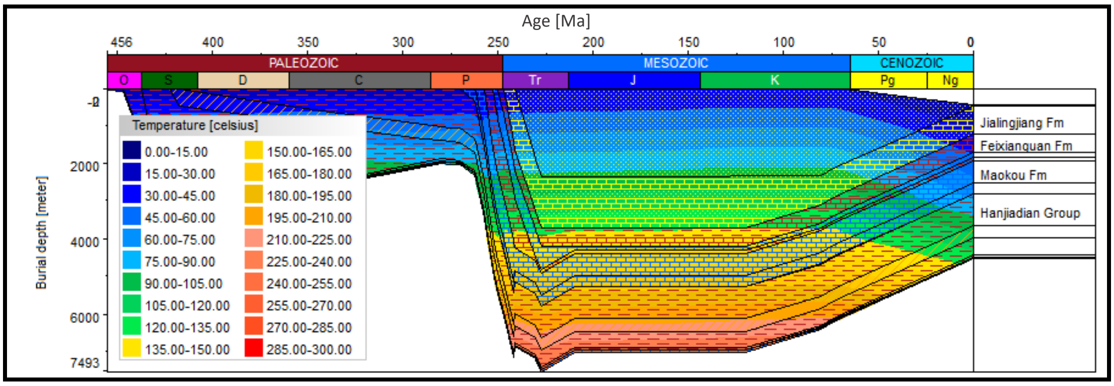

Fig. 8: The petroleum system of the Nanchuan area showing the formations at each depth, the colour in the figure represents the temperature evolution

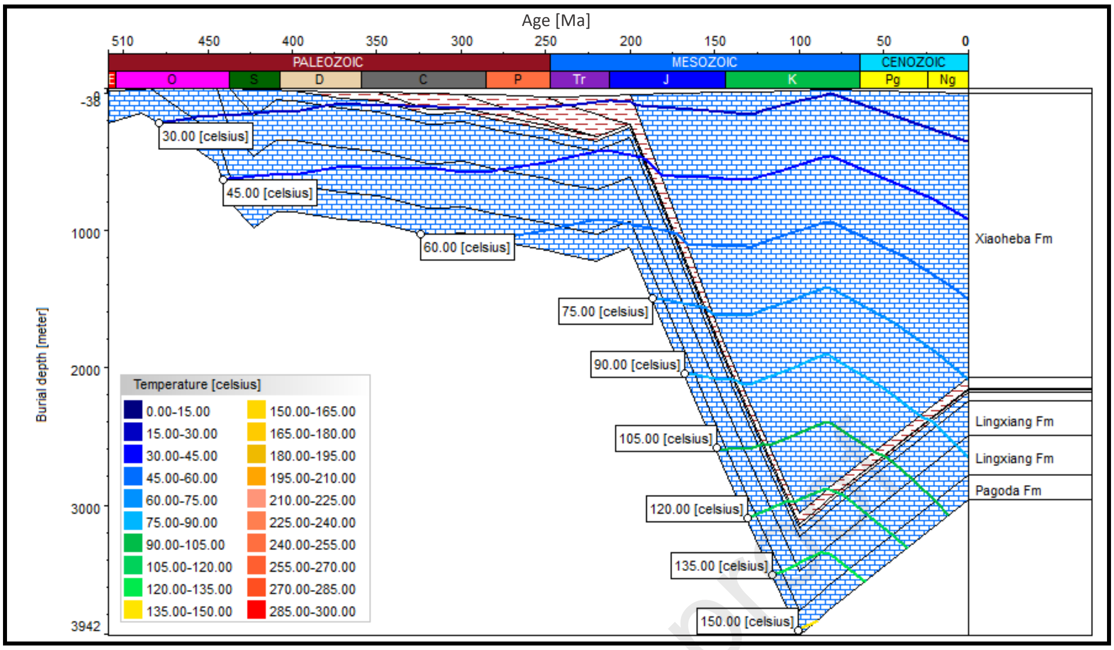

Fig. 9: The petroleum system of the Southeast of Chongqing region obtained from the Pengye 1 well data, the lithology of the Lower Silurian Longmaxi and Upper Ordovician Wufeng formations is shale whereas the remained formations are limestone

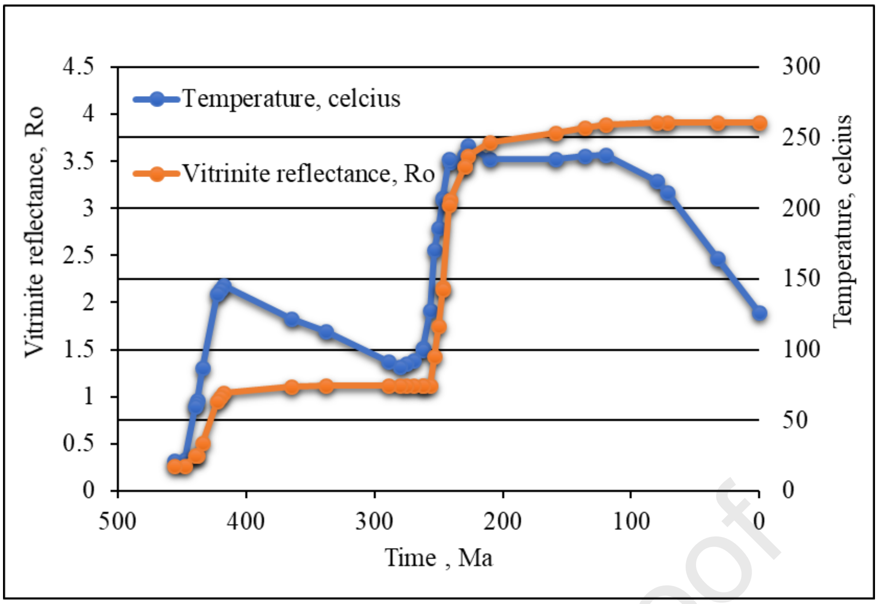

Fig. 10: The history of temperature changes and hydrocarbon maturity in the shale formations of the Nanchuan area

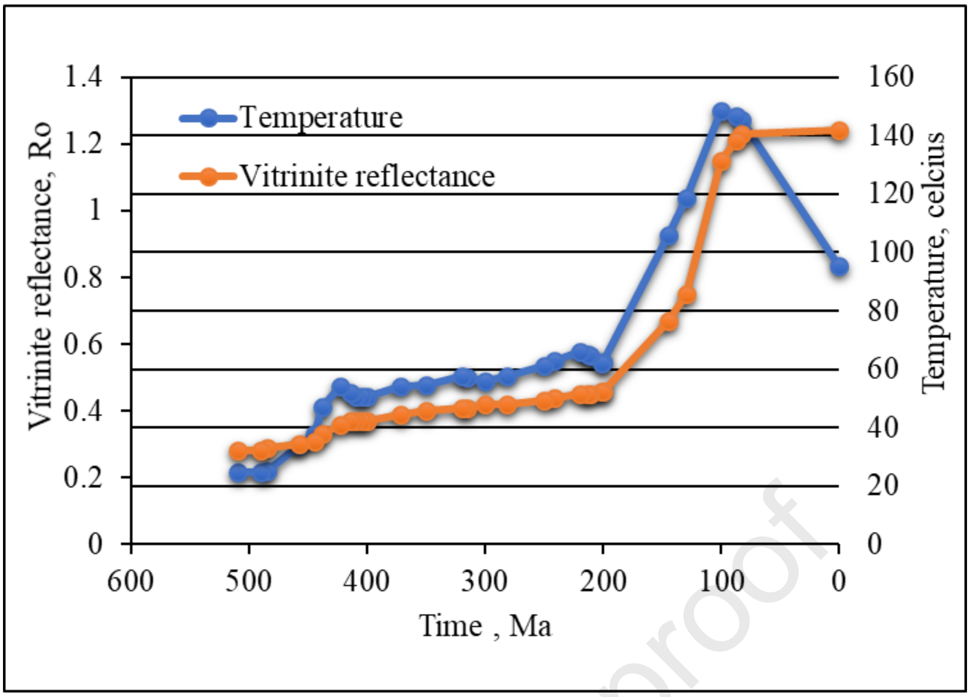

Fig. 11: The relationship of temperature and vitrinite reflectance of Lower Silurian Longmaxi and Upper Ordovician Wufeng Formations in the SE of the Chongqing region

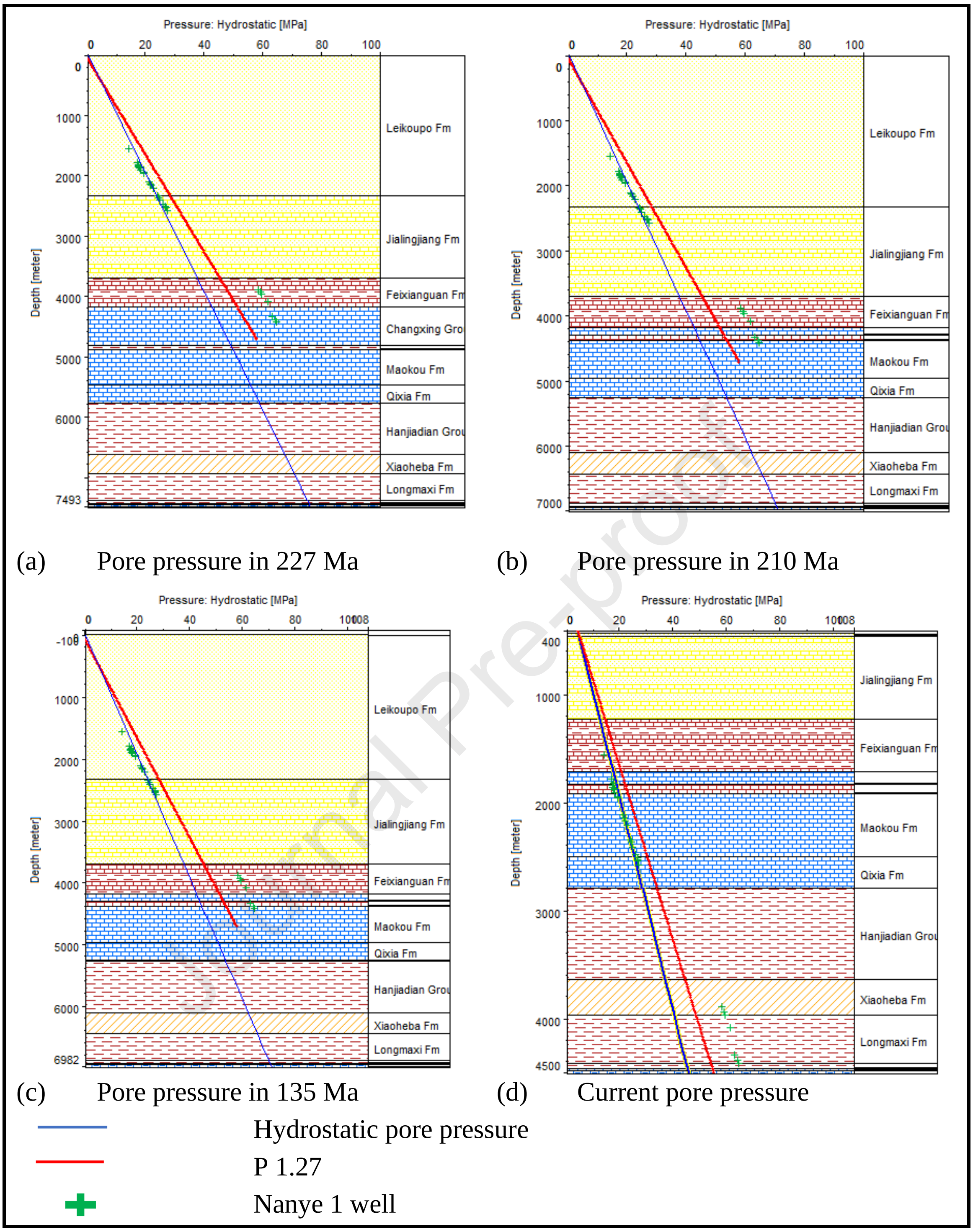

Fig. 12: Pore pressure evolution in the SE of Sichuan Basin, the green data represent the pore pressure in the Nanye 1 well, the red line represents the pore pressure coefficient of 1.27 (above this coefficient the region is overpressured), the blue line represents the hydrostatic pore pressure

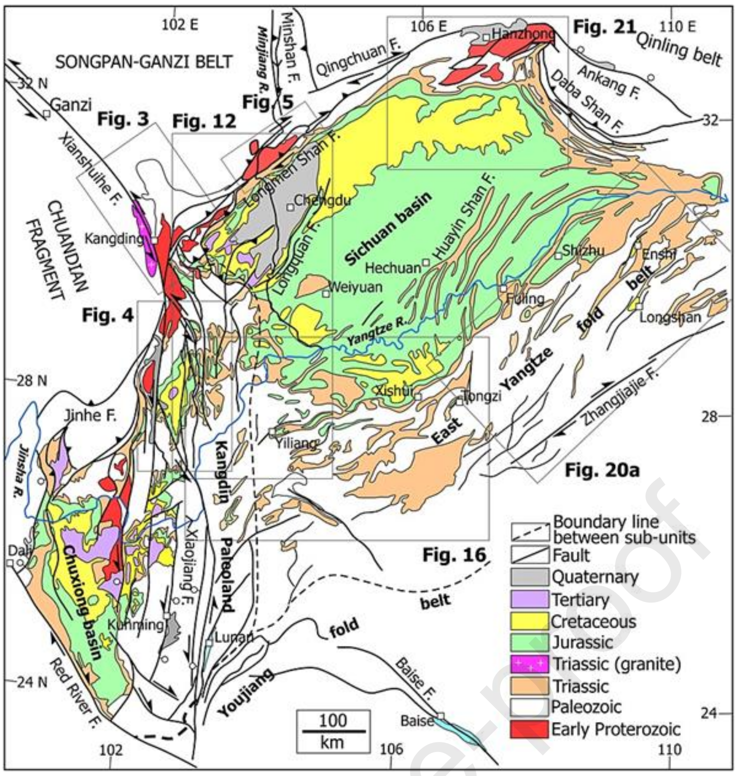

Fig. 13: A geologic map showing the major faults system (boundary faults) found in the Sichuan basin (Wang et al., 2014)

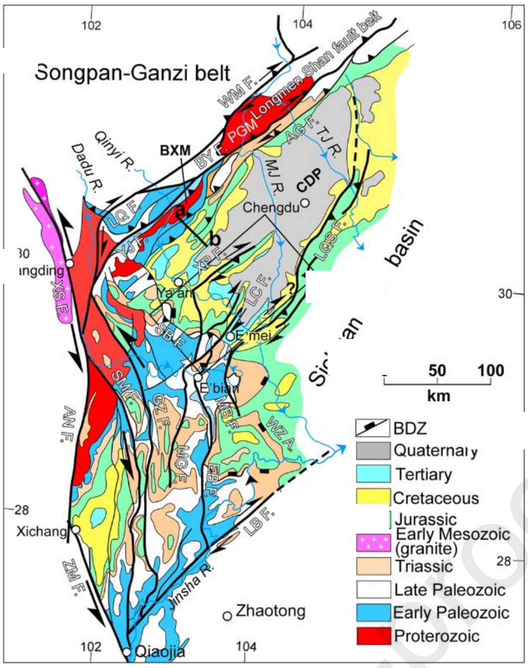

Fig. 14: The active and basement faults in the Sichuan Basin, changling banbianshan fault (CB-F), fangdoushan fault (FDS-F), lianfeng fault (LF-F), longquanshan fault (LQS-F), pujiang-xinjin fault (PX-F), yingjing mabian yajin fault (YMY-F), zhaotong fault (ZT-F), yingjing mabian yajin (YMY), changing (CN), leibo (LB), leshan (LS), mabian (MB), qianwei (QW), rongchang (RX), suining (SN), tongjing (TJ), tongnan (TN), wulong (WL), wiyuan (WY), xingwen (XW), yibin (YB) and yanjin (YJ) as indicated in the figure (Lei et al., 2020; Wang et al., 2014)

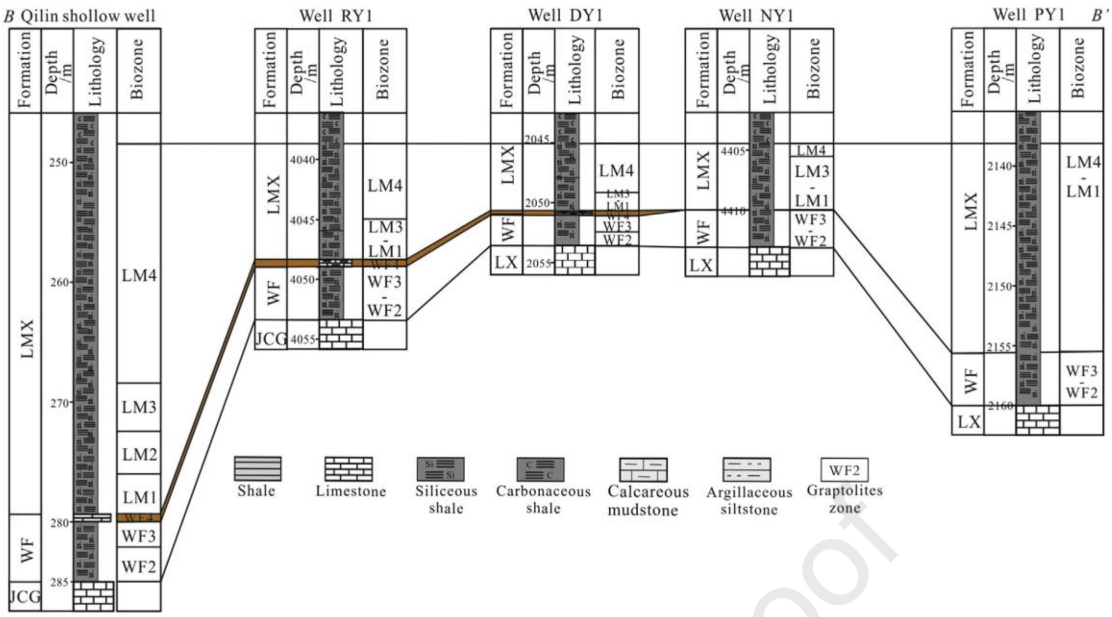

Fig. 15: The depth of Longmaxi (LMX) and Wufeng (WF) Formations in the Nanye 1 (NY 1) and Pengye 1 (PY 1) well, respectively, in the Southeastern Sichuan basin (Nie et al., 2017)

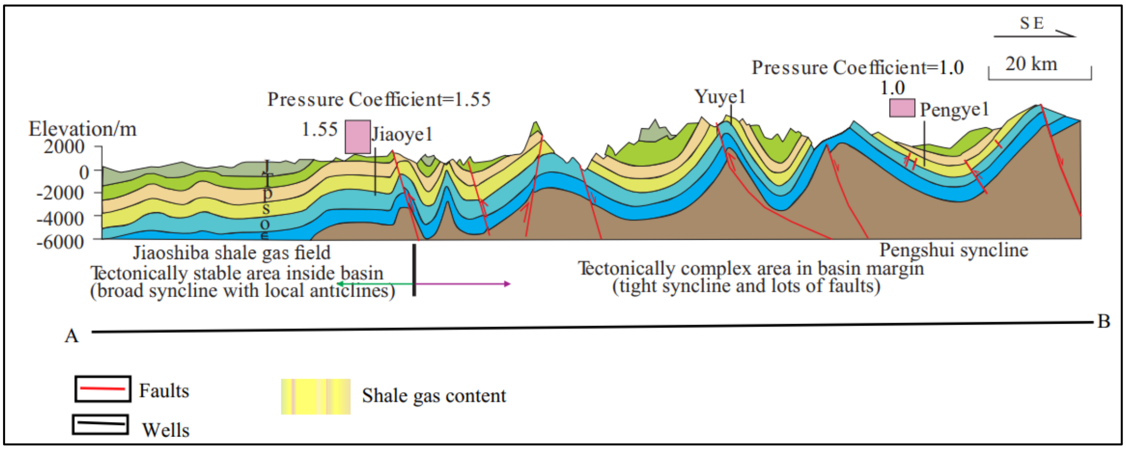

Fig. 16: Cross-section A-B of Fig. 1 shows the faults found in the Pengshui Area, SE of the Chongqing region (Zhang et al.,2018)

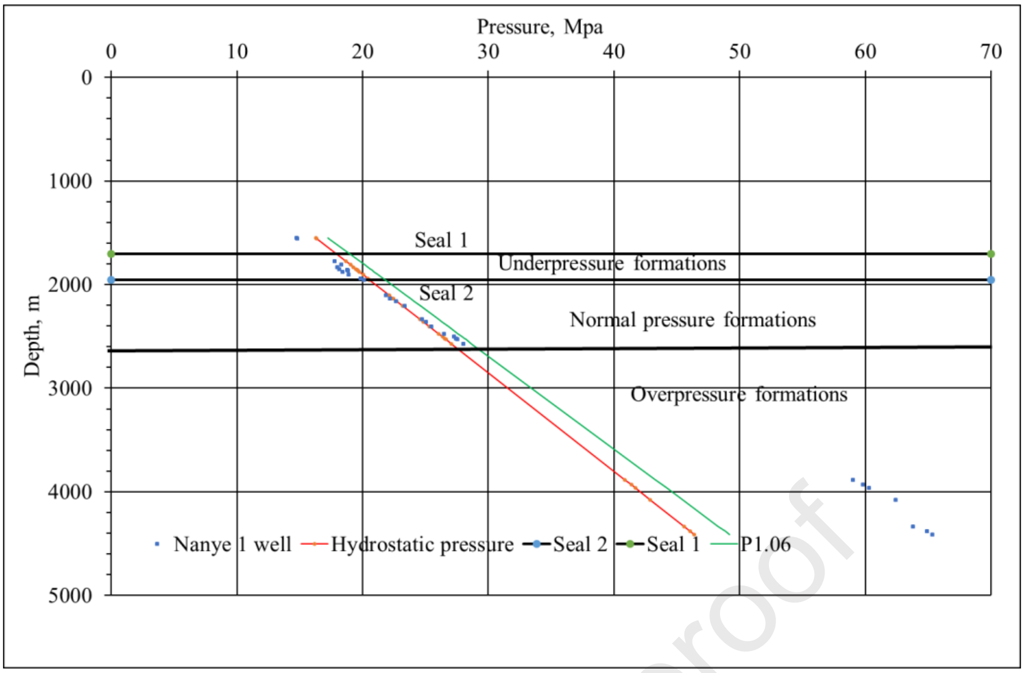

Fig. 17: The pore pressure-depth profile in the SE Sichuan basin, Seal 1 represents the low permeable rock found above the underpressured formations, Seal 2 represents the low permeable rock below the underpressured formations, P1.06 is the region with a pore pressure coefficient of 1.06, Nanye 1 well represents the pore pressure data in the formations

Highlights

The article is concerned with the identifications of normal to underpressure formations

Methods including determination of pressure coefficient and pressure depth plot were used in identifying the normal to underpressure formations. Whereas basin modelling, studying the effect of uplift and erosion by a mathematical model, studying the faults system in the basin were used to identify the origins of normal and underpressure formations.

Three formations, Upper Permian Longtan and Middle Permian Maokou formations in the Nanchuan area, and Lower Silurian Longmaxi formations in the Pengshui area, southeast of Chongqing region were identified as normal to underpressure formations.

The origins of these normal and underpressure formations were temperature decrease, the rebound of the rock porosity, and migration of the gas from the formation through the faults.

Tectonic uplift and erosion, and the presence of faults were identified as the main factor which influences the formation of these normal to underpressure formations.

The presence of seal rock was mentioned as the main factor which helped in the conservation of pressure in these formations.

Declaration of interests

☒ The authors declare that they have no known competing financial interests or personal relationships that could have appeared to influence the work reported in this paper.

☐The authors declare the following financial interests/personal relationships which may be considered as potential competing interests: